EVALUATING SPECIES-SPECIFIC NAUPLIAR RECRUITMENT DURING THE WINTER-TO-SPRING TRANSITION IN THE NORTHERN GULF OF ALASKA USING MOLECULAR TOOLS

A THESIS SUBMITTED TO THE GRADUATE DIVISION OF THE UNIVERSITY OF HAWAIʻI AT MĀNOA IN PARTIAL FULFILLMENT OF THE REQUIREMENTS FOR THE DEGREE OF

MASTER OF SCIENCE

IN

OCEANOGRAPHY

AUGUST 2024

By

Lauren N. Block

Thesis Committee:

Petra H. Lenz, Chairperson
Erica Goetze
Russell R. Hopcroft
Jeffrey C. Drazen

Keywords: nauplii, copepod, Gulf of Alaska, DNA metabarcoding, phenology

1 ACKNOWLEDGEMENTS

First and foremost, I would like to thank my advisor, Petra Lenz. It is difficult to succinctly express all the ways you have played an integral role in my growth both as a scientist and as a person over the past six and a half years. Thanks for believing in me and pushing me to become a better critical thinker, leader, storyteller, and overall better person. I would also like to thank my committee members, Russell Hopcroft, Erica Goetze, and Jeffrey Drazen for their careful review, feedback, and enthusiasm for my research. This research project was funded by NSF #2222376, #1756767, and #2222592. Winter field collections were made possible by a team of wonderful people including Petra, Dan, Angie, Vittoria, Michelle, and Jennifer. Thank you for braving the cold in the name of science and making the winter enjoyable. Angie, thank you for being the best right-hand women both in Seward and at home. Many thanks to Russ, Caitlin, Alex, and the Hopcroft lab for logistical support, training, supplemental samples, processing the formalin samples, and adopting me into your lab. Thank you, Suzanne Strom and Kerri Fredrickson, for your assistance with phytoplankton sampling design and providing supplemental data. Thanks to Brian for your excellent captain skills and bad movie recommendations, Pete for the training and trivia, and the Seward Marine Center folks for your hospitality. Many thanks to the Hartlenz lab for enduring my endless supply of graphs, Dan and Ann for your questions that make me think, Matt for your bioinformatic training, Tehya for your ImageJ skills, Kira for teaching me to love fieldwork, Lynn for your morning greetings and keeping track of everything, and the folks in PBRC for being a great community. Thanks to Karen Selph and the SOEST Flow Cytometry Facility for analyzing flow cytometry samples and providing the setup and training for processing Lugol's samples. Many thanks to Allexa Burger, Christy Handel, and Jennifer Saito for your molecular wisdom and the MGAL and ASGPB facilities for sample processing and sequencing. Thanks to Kristin Momohara and the Oceanography department for your support. I am grateful for the many colleagues and friends I

have gained through my time with the Oceanography department, NGA LTER, and EcoFOCI program. Lastly, I would like to thank Mom, Dad, Hannah, and extended family for being the most loving and supportive family I could ask for. Austin, thank you for your constant encouragement. To my friends, you bring so much joy into my life and I am very grateful for you all.

2 ABSTRACT

The Gulf of Alaska is a highly seasonal environment that is characterized by an order-of-magnitude increase in copepod biomass in the photic zone between winter and spring. Copepod recruitment processes, including the location and timing of naupliar production, responsible for the transition from low-biomass winter conditions to the highly productive spring are not well characterized. The recruitment patterns of copepod nauplii were examined in Resurrection Bay, Alaska using biweekly sampling between January and March with zooplankton collected from three depth strata. Nauplii were identified using DNA metabarcoding and species-specific naupliar phenologies were contextualized with environmental data and copepodite and adult copepod population data. This study revealed that nauplii were abundant throughout the winter and were comprised of a diverse assemblage of species. The community composition changed over the course of the season, with different copepod species exhibiting three distinct naupliar phenologies. These include species with nauplii that were 1) present during the winter and absent during the spring, 2) absent during the winter and present during the spring, and 3) present during both winter and spring. Several closely related species were split across groups, revealing temporal niche partitioning of reproduction and naupliar phenologies. For most species in the third group, the presence of nauplii during the winter occurred despite the absence of ovigerous females. While ovigerous females may have been missed or the nauplii could have been sourced from reproductive populations outside of Resurrection Bay, it is also possible that some copepods overwinter as nauplii. Prior to the spring phytoplankton bloom, a moderate increase in chlorophyll α concentrations occurred during March, coinciding with a period of female maturation, an increase in naupliar abundances, and the appearance of later developmental stages. These observations suggest smaller increases in chlorophyll prior to the large spring bloom may be critically important to recruitment of copepod nauplii, their survival, and their growth.

3 TABLE OF CONTENTS

4 LIST OF TABLES

5 LIST OF FIGURES

6 INTRODUCTION

The Gulf of Alaska is a high-latitude marine environment that experiences large seasonal variations in light, temperature, salinity, vertical mixing, and nutrient availability (Childers et al., 2005; Royer, 1974; Stabeno et al., 2004). These seasonal changes lead to annual cycles of low and high productivity. The spring is characterized by a large phytoplankton bloom driven by an increase in light, stratification, and availability of nutrients (Behrenfeld, 2010; Brickley and Thomas, 2004; Strom et al., 2006, 2016; Sverdrup, 1953). The spring bloom supports large populations of zooplankton, fish, marine mammals, and seabirds— enabling subsistence harvesting, large commercial fisheries, and tourism (Cooney et al., 2001; Coyle and Pinchuk, 2003; Doyle et al., 2019; Strom et al., 2019).

In contrast, the winter is characterized by cold temperatures, low light, and deep mixing of the upper water column (Stabeno et al., 2004). Chlorophyll α concentrations reach an annual minimum (<0.5 mg/m^3) during the winter (Brickley and Thomas, 2004; Childers et al., 2005; Waite and Mueter, 2013). Copepods, which typically dominate the zooplankton biomass in the upper 100 m, are at their lowest annual abundances during the winter—often one to two orders of magnitude lower than their spring biomass (Cooney et al., 2001; Coyle and Pinchuk, 2003). In Prince William Sound, Alaska, copepod abundances are between 100-500 copepods per cubic meter during the winter with biomass at less than 0.01 g/m^3 in the upper 50 m (Cooney et al., 2001; McKinstry and Campbell, 2018). The surface copepod populations are typically comprised of smaller copepods like *Oithona*, *Pseudocalanus*, and *Acartia* with diapausing *Neocalanus and Calanus* expected to be present at depth (Cooney et al., 2001; McKinstry and Campbell, 2018; Miller and Clemons, 1988; Peterson, 1979).

The 10-fold increase in copepod biomass between March and May has been attributed to the reproduction of the overwintering populations, and the survival and growth of the next

generation of copepod nauplii (Coyle and Pinchuk, 2003). While long-term programs have monitored spring copepod populations, copepod life histories and reproduction during the winter-to-spring transition remain poorly understood (Hopcroft, 2021; Sousa et al., 2016). This is due to limited winter sampling and little information on the early developmental stages (nauplii), which are challenging to identify morphologically. In the Gulf of Alaska, few studies include zooplankton collections made prior to April, with even fewer reporting naupliar abundances (Coyle and Pinchuk, 2003; Paul et al., 1991). Furthermore, most winter zooplankton collections are limited to the upper 50 or 100 m and use nets with mesh sizes that exceed 200 μm, which can miss smaller zooplankton and nauplii (Cooney et al., 2001; Coyle and Pinchuk, 2003; Hopcroft et al., 1998; McKinstry and Campbell, 2018; Nichols and Thompson, 1991). Instead, much of what is understood about copepod winter life histories is based on spring and fall species characteristics as well as studies conducted outside the Gulf of Alaska. Copepod naupliar recruitment patterns need to be investigated in order to establish species-specific life-history and reproductive strategies in the Gulf of Alaska, characterize the winter food web, and predict how winter environmental forcing might impact copepod populations.

Three patterns of copepod reproductive phenologies were proposed by Heinrich based on a review of species' feeding ecologies and seasonal copepodite stage distributions (Heinrich, 1962). The three patterns are 1) reproduction independent of the spring bloom often occurring in the winter, 2) reproduction closely tied to the spring bloom, and 3) year-round reproduction with increased brood size during the spring bloom. While the patterns outlined by Heinrich (1962) provide a useful framework for the timing of species-specific naupliar recruitment, they were not substantiated by winter sampling. Nevertheless, group membership among the three patterns can be expected to be dependent on a species' reproductive strategy. Income, capital, and hybrid breeding are different reproductive strategies found among copepods in high-latitude ecosystems (Jönsson, 1997; Sainmont et al., 2014; Varpe et al., 2009). The three strategies

differ in their reliance on energetic input from feeding to fuel reproduction and are therefore hypothesized to control the timing of naupliar recruitment in relation to the timing of the spring bloom.

Income breeding is characterized as reproductive output fueled by active feeding and is closely tied to periods of high food availability (Jönsson, 1997). Therefore, the presence of nauplii from income-breeding copepods is expected to be synchronized with the spring bloom (Heinrich's second pattern). Reproduction is tightly coupled with the availability of food resources for most copepod species (Mauchline, 1998). In the Northern Gulf of Alaska, the genera *Oithona*, *Pseudocalanus*, *Acartia*, and *Metridia*, are considered income breeders and they are abundant through much of the spring and summer (Castellani et al., 2007; Hopcroft et al., 2005; Napp et al., 2005; Peterson et al., 1991). During the winter when prey availability is low and income-breeding species are food-limited, egg production is predicted to be low and their nauplii mostly absent. As the season progresses towards the spring and phytoplankton concentrations increase, income-breeding species are expected to become reproductively active with an associated increase in income-breeding nauplii. Because the majority of copepod species are income breeders, total naupliar abundances are expected to peak during the spring bloom, as has been previously reported in Resurrection Bay, Alaska (Paul et al., 1991).

Capital breeding is described as reproduction fueled by stored energy, which decouples reproduction from the food source in time and/or space (Jönsson, 1997; Varpe et al., 2009). Therefore, it is hypothesized that nauplii of capital breeding species will align with Heinrich's (1962) first phenological pattern. In the Gulf of Alaska, *Neocalanus* spp. are obligate capital breeders as the females are nonfeeding (Miller et al., 1984; Monell et al., 2023; Roncalli et al., 2020). Juvenile *Neocalanus* copepodites are abundant during the spring bloom, when they store energy in the form of lipids to fuel reproduction (Cooney et al., 2001; Coyle and Pinchuk, 2003;

Lenz and Roncalli, 2019). The fact that reproduction in *Neocalanus* is not tied to the spring bloom allows females to spawn during winter at depth following diapause (Kobari and Ikeda, 2001; Miller and Clemons, 1988; Tsuda et al., 1999). Thus, nauplii of *Neocalanus* are expected to be abundant in the winter and then decrease towards the spring as they develop into copepodites preceding the spring bloom. In April, copepodites are found primarily in the upper 100 m, however little is known about the timing of the ontogenetic migration of the nauplii from depth to the surface waters (Fujioka et al., 2015; Kobari and Ikeda, 2001; Miller and Clemons, 1988).

The third phenological pattern of year-round reproduction aligns best with tropical copepod species that experience less seasonality in phytoplankton growth (Heinrich, 1962). However, there may also be high-latitude copepods that maintain year-round reproduction. These are likely comprised of species not limited by phytoplankton production, such as income-breeding species tolerant to low food conditions (e.g. *Oithona similis*), predatory species (e.g. *Paraeuchaeta* spp.), or those with hybrid breeding strategies (Baier and Napp, 2003; Nakatani, 1995; Wiborg, 1954; Zamora-Terol et al., 2013). The hybrid reproductive strategy is defined narrowly here as the ability to produce at least one clutch of eggs using lipid reserves followed by a switch to income breeding when food resources increase, as observed for *Calanus glacialis* in the Arctic Atlantic (Niehoff et al., 2002). The reproductive strategy for the closely-related *Calanus marshallae* in the Gulf of Alaska remains ambiguous with some studies suggesting it is an income breeder while others indicating a more hybrid strategy (Baier and Napp, 2003; Peterson, 1979; Vidal and Smith, 1986).

Based on the framework outlined above, it is hypothesized that nauplii of the capital-breeding *Neocalanus*. would be present during the winter (Heinrich's pattern one). Nauplii of income-breeding species, including those from the genera *Pseudocalanus*, *Acartia*, and *Metridia*, are

not expected to be present until phytoplankton concentrations increase (Heinrich's pattern two). Finally, nauplii of *Oithona*, *Paraeuchaeta elongata*, and *C. marshallae* (if it utilizes a hybrid strategy) are hypothesized to be present during the full sampling period (Heinrich's pattern three). To test these hypotheses, biweekly sampling was combined with the application of DNA metabarcoding to identify nauplii and describe the timing and depth of naupliar recruitment for copepod species. Species-specific naupliar phenologies were examined and placed in context with environmental data, phytoplankton prey field, copepodite populations, and the presence of ovigerous females.

7 METHODS

7.1 STUDY SITE

Field sampling was conducted in Resurrection Bay, located in south-central Alaska, with a maximum depth of nearly 300 m (Heggie et al., 1977). The inner fjord is separated from the outer fjord and the greater Gulf of Alaska by a relatively shallow sill (185 m depth) that isolates the bottom waters and limits the exchange of deep water during the winter (Heggie and Burrell, 1981). Samples were collected within the inner basin at RES2.5 (60° 1.5' N, 149° 21.5' W; 298 m deep), an established oceanographic station (Figure 1) (Heggie et al., 1977; Paul et al., 1991). The protection of the fjord and ease of access from the Seward Marine Center (Seward, AK) allowed for routine winter sampling and access to diapausing *Neocalanus* and *Calanus* at depth, as determined during preliminary collections in August and September despite a maximum depth that is shallower than expected diapause depths (>300 m) (Personal observation and Hopcroft personal communication) (Lenz and Roncalli, 2019; Miller and Clemons, 1988). Diapausing copepods were expected to remain in Resurrection Bay through the winter and into the spring, as deep-water renewals are completed between September and October and do not resume until April or May (Heggie and Burrell, 1981).

7.2 FIELD COLLECTIONS

Samples were collected approximately biweekly aboard the R/V *Nanuq* between January 5th and March 24th, 2023 (Table 1). Vertical profiles of water temperature, salinity, and fluorescence were measured from 280 m to the surface using a CTD (SBE25 SeaLogger) and WetLabs chlorophyll α fluorometer mounted on an SBE55 rosette with six 4-L Niskin Bottles. Water was collected at discrete depths (surface, 10, 20, 30, 40, 50, 150, and 280 m) for characterization of the phytoplankton and microzooplankton community. Two casts were required to collect all

water samples. Methods for preservation and processing of chlorophyll α, flow cytometry, and acid Lugol's sample are detailed below.

Zooplankton were collected from three depth strata corresponding to the established RES2.5 surface sample protocol (0-100 m), an intermediate depth (100-200 m), and a deep sample below the sill depth (200-280 m). Surface samples were collected using an elongated QuadNet net equipped with two 53-µm and two 150-µm mesh nets (25 cm diameter) towed vertically from 100 m to the surface as described in Hopcroft (2021). Only the 53-µm nets were used to ensure adequate naupliar retention (Hopcroft et al., 1998; Nichols and Thompson, 1991). Intermediate and deep samples were collected with duplicate 30-cm bongo nets equipped with 53-µm mesh nets towed vertically from near bottom (~280 m) for the deep sample, and from 200 m for the intermediate sample. A General Oceanics double trip mechanism with a messenger weight was used to close the net at the minimum depth (200 m and 100 m for deep and intermediate samples, respectively) before returning the net to the surface. General Oceanics flowmeters were mounted at the opening of each net to measure the volume of water filtered. Net collections were split quantitatively using a Folsom plankton splitter for multiple applications and samples were preserved as described below. Supplemental surface zooplankton samples were collected at RES2.5 using the QuadNet in December 2022, April 2023, and May 2023 aboard either the R/V *Nanuq* or the R/V *Sikuliaq* (Table 1).

7.3 ENVIRONMENTAL SAMPLE PROCESSING

The prey field was characterized using four methods—*in-situ* chlorophyll α fluorescence profiles, size-fractionated extracted chlorophyll α fluorescence, flow cytometry, and acid Lugol's samples. *In-situ* fluorescence profiles provide a high-resolution continuous depth profile and are useful for describing relative vertical and temporal patterns in chlorophyll fluorescence (Figure 2E&F). Chlorophyll α (Figure 3), flow cytometry (Figure 4), and acid Lugol's samples (Figure 5)

were collected at discrete depths. Chlorophyll α samples were size fractionated to estimate the chlorophyll α contribution of pico- and nano-phytoplankton (< 20 μm size fraction) and larger phytoplankton (including diatoms plus larger photosynthetic dinoflagellates) (> 20 μm size fraction). Picophytoplankton were further characterized using flow cytometry, which allowed for the estimation of *Synechococcus* and photosynthetic picoeukaryote biomass. Diatoms, dinoflagellates (both photosynthetic and non-photosynthetic), and ciliates were quantified from acid Lugol's preserved samples. All measurements provide insight into potential prey sources for copepods and their nauplii.

Chlorophyll α was measured at 10-m intervals from the surface to 50 m for each sample timepoint. Supplemental samples taken by collaborators from the NGA LTER program for the December 2022, April 2023, and May 2023 timepoints were included in this analysis. Polycarbonate (47-mm diameter, 20-μm pore size) and glass fiber (25-mm diameter, 0.7-μm pore size) filters were used to size fractionate 250 mL samples using a serial filtration vacuum manifold system (Strom et al., 2016). Filters were extracted in 90% acetone for 24 hours at -20°C in the dark. Fluorescence was measured using a Turner 10-AU fluorometer using the acidification method (Strom et al., 2016). Fluorescence measurements were converted to estimated chlorophyll α concentrations (μg/L) (Lorenzen, 1966). Integrated chlorophyll α (mg/m^2) was calculated using trapezoidal integration (Strom et al., 2016).

Synechococcus, photosynthetic picoeukaryotes, and heterotrophic bacterial abundances were measured using flow cytometry at 8 depths (surface, 10, 20, 30, 40, 50, 150, and 280 m). Samples (1 ml) from each depth were preserved with paraformaldehyde to a final concentration of 0.5%, frozen initially at -40°C, and later transferred to -80°C until batch analysis. Samples were thawed, stained with Hoechst 34580 (1 μg/mL final concentration), and analyzed with a Beckman Coulter CytoFLEX S flow cytometer (Selph, 2021). Data were processed using

FlowJo software (version 10.8.2). *Synechococcus* and picoeukaryote abundances were converted to carbon biomass using cellular carbon content estimates appropriate for the region (200 and 1,490 fg C per cell, respectively) (O'Hara, 2023; Strom et al., 2016).

Microzooplankton samples were collected at 3 depths (50, 150, and 280 m) by gently draining 250 mL of seawater from the Niskin bottle with a silicon tube to avoid bubbling. Samples were then preserved with acid Lugol's solution to a final concentration of 5% (Strom et al., 2019). Glass was added to saturate silica and prevent dissolution of diatoms. Samples were gently mixed and 100 mL subsamples were settled onto microscope slides. Diatoms, dinoflagellates, and ciliates were identified to lowest taxonomic classification, enumerated, and imaged under an inverted microscope. Linear length and widths of cells were measured for a subset of 5 cells (or maximum number) per sample per taxon. Biovolume was estimated using the median linear measurements per taxon and biovolume was calculated using the volumetric equations most closely matching the cell shape (Hillebrand et al., 1999). Biovolume was then converted to carbon biomass according to established diatom and protist carbon:volume relationships (Menden-Deuer and Lessard, 2000).

7.4 ZOOPLANKTON SAMPLE PROCESSING

7.4.1 Preservation

Zooplankton tows included two paired 53-µm nets per depth stratum. The first paired 53-µm net was preserved immediately in 10% formalin for later microscopic analysis. Formalin samples were not size fractionated. The second paired 53-µm net was diluted with 4 L of surface-collected seawater, stored in a dark cooler, and processed on shore within 4 hours. Samples were split into four quarters using a Folsom plankton splitter—one quarter for bulk community DNA metabarcoding and the other quarter for microscopy and individual DNA analysis. The remaining half of the sample was used in other project applications. Each quarter was size

fractionated using Nitex mesh sieves to separate nauplii (53-210 μm), smaller copepod taxa and early copepodites of larger copepod taxa (210-560 μm), and late copepodite and adult stages of larger copepod taxa (>560 μm) based on stage sizes and *a priori* pilot testing (Doyle et al., 2019; Nichols and Thompson, 1991; Peterson, 1979). Each size-fractionated sample was preserved in 95% ethanol and exchanged after 24 hours, following established protocols (Bucklin, 2000).

Ethanol-preserved samples from multiple dates and depth strata were examined under a dissection microscope to determine the stage separation for different copepod species across the size fractions. Size fractionation was designed to prioritize separation of naupliar stages from copepodite and adult stages within the large copepod taxa including *Calanus*, *Neocalanus*, and *Metridia*. The smallest size fraction did not reliably exclude copepodite stages of smaller copepod taxa, including *Oithona*, *Triconia*, and *Pseudocalanus*. Full species-specific stage retention of the size fractions is summarized in table 2. The small (53-210 μm) and medium (210-560 μm) size fractions were analyzed using DNA metabarcoding. They are hereafter referred to as the “small” and “medium” size fractions, respectively. Due to the overwhelming presence of copepodites and adult copepods and absence of nauplii, the > 560 μm “large” size fraction was not analyzed.

7.4.2 Formalin samples

One set of formalin samples collected at monthly intervals from all depth strata were analyzed between January and April (n = 7, Table 1). Preserved samples were sequentially split using a Folsom plankton splitter until the smallest subsample contained approximately 100 of the most abundant taxa. Individuals were identified to lowest taxonomic classification and enumerated. Subsequent subsamples were processed to enumerate less abundant taxa until sufficient counts were reached. Copepod nauplii were enumerated and classified to Order. Copepodites

were staged and ovigerous females were quantified. Ovigerous females were defined as females with either visible eggs developing inside their ovary or the presence of external egg sacs. Individual lengths were measured and established length-weight regressions were used to estimate biomass (Hopcroft and Clarke Hopcroft, 2019).

7.5 DNA METABARCODING

DNA metabarcoding was conducted on two types of samples—size fractionated total community (hereafter referred to as bulk community samples) and hand-sorted cohorts of nauplii (hereafter referred to as naupliar cohort samples). For bulk community samples, the small and medium size fractions for each biweekly timepoint and depth stratum were processed (Table 1). Ethanol was drained from the sample using a clean 53-µm sieve, sample biomass was weighed, and DNA was extracted with the Qiagen DNeasy Blood and Tissue Mini Column kit. DNA was extracted following the manufacturer's protocol with an extended 24-hour proteinase K incubation to ensure adequate lysis.

Preliminary analysis revealed the presence of nauplii from small copepod species. However, both copepodites and nauplii of the small species were retained in the 53-210 µm size fraction (Table 2). Therefore, naupliar cohort samples were used to better characterize the contribution of small copepod taxa to the naupliar community. Cohorts of 100 nauplii were hand-sorted under a dissection microscope for one sample per month (except for the December 28th sample, which contained 150 nauplii) and all depth strata, where applicable (Table 1). A random subsample was taken from a well-mixed ethanol-preserved sample using a Hensen Stempel pipette and the first 100 nauplii were selected. To prevent bias, all nauplii were removed within a visual field before moving the Petri dish for additional nauplii. For these small-sized samples, DNA was extracted using the Zymo Research Quick-DNA™ Miniprep Plus Kit following manufacture's protocols with an extended 12-hour proteinase K incubation.

Eluted DNA concentrations were measured using a Thermo Scientific™ NanoDrop™ spectrophotometer and normalized to 5 ng μL^{-1} prior to PCR amplification. The mlCOIintF and jgHCO2198 primers (mlCOIintF 5'-GGWACWGGWTGAACWGTWTAYCCYCC-3'; jgHCO2198 5'-TAIACYTCIGGRTGICCRAARAAYCA-3'), commonly used in zooplankton metabarcoding applications, were used to amplify a 313 bp region of the mitochondrial cytochrome *c* oxidase subunit I (mCOI) gene (Leray et al., 2013; Matthews et al., 2021; Questel et al., 2021). Amplification of the targeted gene was done using PCR in 20-µL volumes using the ultrahigh-fidelity ThermoFisher Invitrogen™ Platinum™ II *Taq* Polymerase and Hot-Start PCR Master Mix with 5 µL of the normalized DNA samples. The PCR was run with an initial denaturation step at 94°C for 3 min followed by 28 cycles of 94°C for 15 s, 48°C for 32 s, 68°C for 15 s, and a final extension for 5 min at 68 °C (Matthews et al., 2021). Amplifications were quality-checked for amplicon size using gel electrophoresis. Samples were then purified, indexed, and pooled using Illumina Nextera Library Prep kit and sequenced using Illumina MiSeq (V3 300-bp paired end) at the University of Hawaii ASGPB facility. PCR, sequencing, and downstream bioinformatic processing was completed in separate batches for bulk community samples and naupliar cohort samples.

Bioinformatic processing was done using QIIME2 v.2023.5 (Bolyen et al., 2019). Demultiplexed reads were trimmed, filtered to remove noisy sequences, chimeras, and singletons, and dereplicated using DADA2 (Callahan et al., 2016). Reads were trimmed at the sequence depth in which the sample 25^{th} percentile Phred quality score was below 30. For bulk community samples, forward and reverse reads were truncated at 268 bp and 196 bp, respectively. For naupliar cohort samples, forward and reverse reads were truncated at 273 bp and 220 bp, respectively. Amplicon sequence variants were then clustered into operational taxonomic units (OTUs) based on 97% sequence identity using VSEARCH (Rognes et al., 2016). Samples were rarefied to the lowest sequencing depth (49,804 bp for bulk community samples and 62,893 bp

for naupliar cohort samples). Representative sequences for each OTU were classified and clustered using a Naïve Bayes Classifier (scikit-learn v. 0.24.1) trained using reference sequences from the MetaZooGene database (MZGdb) (Bucklin et al., 2021). The full MZGdb (downloaded July 14, 2023), included global sequences of marine invertebrates, vertebrates, and microbes. The downloaded sequences were compiled, cleaned, dereplicated, and trimmed to the Leray mCOI amplicon region using RESCRIPt, resulting in 150,470 reference sequences used to train the classifier (O'Rourke et al., 2020; Robinson et al., 2021).

7.6 Analysis and Statistics

All data processing, analyses, and visualization were conducted in the R (v4.3.1) programming environment. Data manipulation was done using tidyverse packages and graphs were constructed using ggplot, ggpubr, and ggbreak (Kassambara, 2023; Wickham et al., 2019; Xu et al., 2021).

Empirical cumulative distribution function curves were plotted individually for calanoid and cyclopoid naupliar length distributions. Two-way Kolmogorov-Smirnov tests were used to test for differences in naupliar length distributions among sample dates and depth strata.

A non-metric multidimensional scaling (nMDS) ordination was used to examine differences in community composition among naupliar cohort samples (n = 12, Table 1). nMDS ordinations were constructed using a Bray-Curtis dissimilarity matrix based on relative read composition of all copepod taxa (n = 28) present in the samples. Environmental variables (temperature, salinity, and fluorescence averaged across the depth strata and numeric day of year) and community diversity metrics (species richness, Simpson's diversity, and Pilou's evenness) were correlated with sample position in two-dimensional space. Vectors point in the direction of steepest increase. Significant correlations were determined by permutation (n = 999) of tested

parameters and only significantly correlated vectors were plotted. nMDS ordinations and vector fits were constructed using the vegan package (Oksanen et al., 2022).

Cluster analysis using Ward's hierarchical clustering method was used to group species based on phenological patterns from bulk community and naupliar cohort data (Nielsen et al., 2021). Reads were normalized using a Wisconsin double standardization (relative reads per sample divided by total reads for a species; calculated separately for small-size-fraction bulk community and naupliar cohort samples) and summed across depth strata (Kelly et al., 2019). The resulting values provide information on what fraction of total sequences for a given species were found on a particular date. This was done to eliminate potential bias due to differential abundances between species and isolate the seasonal signal. The Wisconsin double standardization behaves identically to the eDNA index developed by Kelly and colleagues, which has been shown to strongly track temporal changes in a species' biomass (Kelly et al., 2019).

8 RESULTS

8.1 ENVIRONMENT

8.1.1 Hydrography

The CTD profiles showed the coldest temperatures and lowest salinities near the surface for each sampling date. Surface temperatures decreased between January and March, reaching a minimum at the end of the sampling period (Figure 2 A&B). This is consistent with previously described wintertime conditions, which reach minimum surface temperatures in March and April (Heggie et al., 1977; Stabeno et al., 2004). Water temperatures ranged from 4.6°C to 7.2°C with the warmest waters in the middle water column (Figure 2A).

The temperature and salinity signatures for the three zooplankton depth strata were distinct and exhibited different seasonal patterns. Mean temperatures decreased over time in both the 0-100 m (5.9°C to 4.5°C) and 100-200 m (6.8°C to 5.3°C) depth strata with larger vertical temperature differences in the upper 100 m (Figure 2B). In the 200-280 m depth stratum, water temperatures remained constant with a mean temperature of 6.0°C. Salinity was highest between 200-280 m (average 33.0) and intermediate (average 32.1) between 100-200 m and remained constant over the season at these lower depths (Figure 2 C&D). In the upper 100 m, average salinity increased from 30.7 to 31.6, which is consistent with the region's seasonal pattern of increasing surface salinity leading into spring due to the winter reduction of freshwater input (Heggie et al., 1977; Stabeno et al., 2004). Persistent dense (~26 kg/m^3) bottom waters below the sill depth matches previous descriptions of the inner bay water masses (Heggie et al., 1977).

8.1.2 Prey field

Between late December and late February, prey availability was low and consisted primarily of smaller cells (<20 μm). All prey field indicators showed a moderate increase in the surface

March prey field concentrations, with approximately a three-fold increase in total chlorophyll α prior to the highly productive spring bloom conditions in April and May. Below 100 m, prey field concentrations remained low throughout the season with low *in-situ* chlorophyll α fluorescence, *Synechococcus*, photosynthetic picoeukaryote, ciliate, dinoflagellate, and diatom concentrations (Figures 2E, 4, & 5).

In-situ fluorescence profiles indicated an increase in concentration of chlorophyll α as well as the depth distribution of the chlorophyll over the sampling period, particularly in the upper 100 m (Figure 2E&F). In January, the water column had low chlorophyll fluorescence with the highest fluorescence region in the upper 10 m. Fluorescence increased over time with a pulse of productivity observed on February 7th in the upper 30 m. This was also observed in flow cytometry samples (see below). *In-situ* fluorescence then decreased on February 22nd before the bloom on March 12th which extended to depths of approximately 100 m. A small lens of low-fluorescence water is visible in the top 5 m of the water column, indicating the bloom likely started prior to the March 12th timepoint and is being mixed to deeper depths. Fluorescence then decreased at the surface on March 24th but increased between 100-200 m (Figure 2F). Apart from this last timepoint, fluorescence below 100 m was very low throughout the season.

Between December 28th and February 22nd, concentrations of chlorophyll α were below 0.17 µg/L (Figure 3). The chlorophyll was primarily in the <20 µm size fraction (84±8% of total chlorophyll α; average ± sd), indicating the wintertime phytoplankton community was comprised mostly of small pico- and nano-phytoplankton. Chlorophyll concentrations increased as the season progressed, with a gradual rise in the > 20 um size fraction. On March 12th, chlorophyll α concentrations increased at all sample depths (0-50 m; Figure 3), ranging from 0.24 to 0.32 µg/L, and remained elevated on March 24th. In March, the fraction of chlorophyll in the >20 µm size fraction increased 30±4%, reflecting an increase in diatoms and dinoflagellates (see

below). In April and May, maximum chlorophyll α measurements were almost an order of magnitude higher (3.73 µg/L and 4.69 µg/L, respectively) with the > 20 µm size fraction making up more than 70% of chlorophyll α in the subsurface samples.

Picophytoplankton biomass estimated from flow cytometry was dominated by photosynthetic picoeukaryotes (Figure 4). Across all samples, *Synechococcus* made up between 2 and 26% of total picophytoplankton biomass and remained relatively constant over time. Photosynthetic picoeukaryote biomass was low on January 5th with the highest biomass observed at the surface (0 m) at 4.1 µgC/L and declining to 0.6 µgC/L at 50 m. A four-fold increase in photosynthetic picoeukaryote biomass was observed near the surface on February 7th, consistent with the increase in *in-situ* fluorescence shown in the upper 25 m (Figure 2E). The photosynthetic picoeukaryote biomass then declined in the surface 50 m on February 22nd before increasing again on March 12th (Figure 4). Biomass was similar at all measured depths between 0 and 50 m on March 12th (average of 8.6 µgC/L), further supporting a well-mixed upper water column on March 12th. On March 24th, surface (0 m) biomass remained similar to March 12th but declined with depth.

Ciliate, diatom, and dinoflagellate biomass followed similar trends. Minimum biomass was observed on January 5th with an overall low biomass (0.09 µgC/L at 50 m), which was dominated by diatoms (85.5%) (Figure 5). Ciliate and dinoflagellate biomass was very low at that time. Ciliate biomass remained low through March, not exceeding 0.1 µgC/L. Total biomass of dinoflagellates and diatoms increased by nearly an order of magnitude (1.4 µgC/L at 50 m) on February 22nd with roughly equal contribution of dinoflagellates and diatoms. A three-fold increase in biomass was then observed on March 12th at 50 m with similar relative contributions of diatoms and dinoflagellates, consistent with the observed increase in >20 µm chlorophyll α (Figure 3). Total biomass was lower on March 24th at 50 m but increased at 150 m and 280 m,

suggesting the vertical export of the previous bloom. This is consistent with observed increases in the fluorescence profile and increase in picophytoplankton biomass at depth (Figure 2E & Figure 4). Common diatom taxa observed included *Ditylum brightwelli*, *Rhizosolenia* spp., *Coscinodiscus* spp., and several unidentified chain-forming diatoms.

8.2 CHARACTERIZATION OF THE COPEPOD COMMUNITY

8.2.1 Initial January 5th Community

On January 5th copepod (copepodite and adult stages) abundance and biomass was low in the 0-100 m depth stratum (236 individuals per m^3 and 0.0041 g/m^3), consistent with prior reports of low surface zooplankton abundances and biomass in February and March (Figure 6) (Cooney et al., 2001; Coyle and Pinchuk, 2003; Paul et al., 1991). *Pseudocalanus* and *Oithona* made up 89% of copepod abundances. The remaining 11% included *Metridia pacifica*, *Microcalanus*, *Microsetella norvegica*, and oncaeid cyclopoids. Nauplii were present at abundances four times higher (972 individuals/m^3) than the combined abundance of copepodites and adults in the 0-100 m depth stratum (Figure 6). Although their biomass (0.0008 g/m^3) was less than a quarter of the combined copepodite and adult biomass due to their small size.

The January 100-200 m depth stratum was expected to be similar to the upper 100 m, however copepod abundances were approximately seven times greater than the surface sample (1622 individuals/m^3) (Figure 6). Taxonomically, the community composition was similar to the 0-100 m depth stratum with high prevalence of *Oithona, Pseudocalanus,* and oncaeid cyclopoids including *Triconia borealis*. Biomass was five times greater than the surface samples and consisted of mostly *Oithona* and *M. pacifica*. As expected, *Neocalanus flemingeri* and *Calanus marshallae* were rare in the upper 200 m in early January with abundances below 0.7 individuals/m^3. Naupliar abundance (1476 individuals/m^3) and biomass (0.0011 g/m^3) were slightly greater in the 100-200 m depth stratum in comparison to the top 100 m (Figure 7).

An unexpectedly high number and diversity of copepods were present in the 200-280 m depth stratum on January 5th with an abundance of 5,265 individuals/m^3 and biomass of 0.3611 g/m^3 (Figure 6). While *Neocalanus* and *Calanus* were expected to be the primary copepods present in the deepest stratum, they constituted only 3% of abundance and 54% of biomass. Instead, *Metridia*, *Oithona, Pseudocalanus*, and oncaeid copepods were highly abundant below 200 m. Naupliar abundances were highest in the deep stratum (2,637 individuals/m^3), 97% of which were cyclopoid nauplii (Figure 7). Total naupliar biomass (0.0011 g/m^3) was similar to the 100-200 m depth stratum biomass despite higher abundances, likely due to the larger proportion of smaller cyclopoid nauplii.

8.2.2 Progression of the naupliar community

In February, the vertical distribution of nauplii was weakly bimodal and became more pronounced in March with low abundances (< 200 individuals/m^3 and 0.0005 g/m^3) in the 100-200 m depth stratum in comparison to those above 100 m and below 200 m (Figure 7). After an initial decrease in naupliar abundances from early January to late February, there were significant increases in naupliar abundances in the 0-100 m and 200-280 m depth strata during March and April. In March, naupliar abundances in the surface 100 m increased to 2,258 individuals/m^3 that corresponded to a 40-fold increase in biomass (0.0053 g/m^3). This was largely due to an increase in calanoid naupliar abundance and the presence of the larger late naupliar developmental stages (Figure 9A). Likewise, naupliar abundances below 200 m increased (3445 individuals/m^3) but was primarily comprised of cyclopoid nauplii. By April, there was an overall decline in total naupliar abundances between 0-100 m with a large decrease in calanoid abundances while cyclopoid naupliar abundances increased (Figure 7).

Naupliar length distributions were measured as an indicator of growth (Figure 8). In January and February, the size distribution of calanoid nauplii was unimodal with no significant differences

between the two months (K-S two-sided Test, $p_{Jan05:Feb22} = 0.294$; Table 3). Mean calanoid naupliar length was 203 ± 52 µm in January and 206 ±76 µm in February. By March and April, mean calanoid naupliar lengths increased and became bimodally distributed with peaks at approximately 150 µm and 350 µm (K-S two-sided test, $p_{Feb22:Mar24} < 0.001$; $p_{Mar24:Apr22} = 0.602$; Table 3). The peak in 350 µm–length nauplii was primarily observed in the 0-100 m depth stratum (K-S two-sided test, $p_{Mar24(0\text{-}100m:100\text{-}200m)} < 0.001$; $p_{Mar24(100\text{-}200m:200\text{-}280m)} = 0.354$; Table 3). Cyclopoid nauplii were on average smaller (145 ± 41 µm) than calanoid nauplii with a unimodal distribution (Figure 8). Significant differences in cyclopoid length distributions across time and depth were observed, however the magnitude of the differences was small (Table 3, Figure 8).

8.2.3 Progression of the copepod community

The diverse overwintering copepod population remained concentrated in the 200-280 m depth stratum (Figure 6). However, total abundance and biomass decreased by 61% and 81%, respectively, between January 5th and March 24th in this depth stratum. *N. flemingeri* biomass declined from 0.0221 g/m^3 to near zero by February 22nd. All other major taxa were present in all samples from January to the end of March. The largest decrease in biomass was due to a 97% decline of *C. marshallae* biomass from 0.1443 to 0.0042 g/m^3 between early January and late March. Samples were not collected below 100 m in April.

In contrast, copepod abundance and biomass increased in the upper 100 m over the sampling period (Figure 6). This could be a result of upward migration of overwintering copepods as well as the recruitment of next generation copepodites. In February, abundance and biomass were still low (354 individuals/m^3; 0.0029 g/m^3) before a sharp increase in late March (1071 individuals/m^3; 0.0169 g/m^3) and April (1949 individuals/m^3; 0.1247 g/m^3). In March, copepod abundances were still dominated by *Oithona*, *Pseudocalanus*, and oncaeid copepods with *Pseudocalanus* and *Neocalanus* contributing the most biomass in the upper 100 m. *Neocalanus*

had the largest increase in biomass between March and April in the upper 100 m (0.0039 g/m^3 and 0.0761 g/m^3, respectively). Other taxa that increased in abundance and biomass between March and April included *Metridia* and *Pseudocalanus.*

In the 100-200 m depth stratum, total abundances decreased initially from January 5th to February 22nd by a factor of three, however, biomass remained relatively unchanged at approximately 0.02 g/m^3. The species composition and contribution to biomass changed with an increase in larger taxa. In addition to *Metridia* contributing largely to the 100-200 m biomass, *C. marshallae* biomass increased approximately 10-fold between January and the later months. However, the increase in 100-200 m biomass does not fully account for the loss of *C. marshallae* biomass at depth.

Despite varying initial overwintering copepodite stage composition among calanoid species, there was a general pattern of species maturation followed by an increase in the number of early copepodites (CI-CIII) between early January and late March (Figure 9). *Neocalanus flemingeri* and *Acartia longiremis* were the only species predominately present as females in early January. On the other hand, January populations for *C. marshallae, Metridia okhotensis, and Pseudocalanus* spp. were dominated by CVs and *Metridia pacifica* was distributed across CV, male, and female stages. By late February, adult female and male stages increased for *M. okhotensis*, *M. pacifica*, and *Pseudocalanus* spp. In contrast, adult *C. marshallae* did not exceed 15% of samples until March 24th. All species except *C. marshallae* showed significant recruitment of early copepodite stages between February and March with copepodite stages comprising greater than 50% of species' populations on March 24th.

8.3 NAUPLIAR COMMUNITY COMPOSITION—MOLECULAR ANALYSES

8.3.1 Sample overview

Bulk community DNA was successfully extracted from the samples (small size fraction: 85±48 mg wet weight; medium size fraction 32±22 mg) and amplified for all 36 samples across six sampling dates collected biweekly from January 5th to March 24th, 2023. Samples include the small (53-210 μm) and medium (210-560 μm) size fractions collected at three depth strata. A total of 3,725,492 reads were generated, of which 2,907,178 contiguous reads were retained (78% retention) following assembly, filtering, denoising, and removal of chimeras. Final assembled reads per sample ranged from 49,804 to 96,529 with an average length of 306 bp. After clustering amplicon sequence variants at 97% identity and removing singletons, there were 1,719 OTUs. Non-metazoan and OTUs unidentified at the Kingdom level were removed (5% of reads), resulting in a total of 2,768,879 metazoan reads comprised of 1,331 OTUs. Samples were rarefied to 49,804 reads and rarefaction curves indicate saturation with between 96 and 254 OTUs per sample (Figure 10). In the small size fraction, 65% of metazoan sequences were annotated as copepods (Figure 11A). Large, small, and unidentified copepods made up 14%, 44%, and 7% of reads, respectively. Sequences of other holoplanktonic and meroplanktonic taxa made up 16% of reads and will not be discussed further. The remaining 19% of reads were not identified past Animalia.

In the small size fraction, reads from large copepod taxa were expected to be contributed entirely by nauplii because copepodite and adult stages were retained by the 210 μm sieve (Table 2). While nauplii of small copepod taxa, including *Oithona* and *Pseudocalanus*, were also present, they were not considered in the analysis of naupliar bulk community composition due to a mix of nauplii and copepodites in the small size fraction. *Neocalanus flemingeri*, *M. pacifica*, and *A. longiremis* were the primary large copepod species present in the small size fraction

samples constituting 49%, 35%, and 9% of total sequences, respectively (Figure 11A). Small amounts of *Neocalanus plumchrus*, *M. okhotensis*, and *C. marshallae* sequences were also present. Species-specific patterns are discussed further below.

A second method was required to assess smaller nauplii since the microscopic analysis revealed the presence of small cyclopoid nauplii (Figure 7). Naupliar cohort samples allowed for the examination of naupliar patterns of all copepod taxa. Furthermore, supplemental non-size-fractionated samples could be included in the cohort analysis, extending the surface-collected timeseries from December 28th, 2022, to May 4th, 2023. The 12 naupliar cohort samples yielded a total of 1,138,396 reads. After filtering, denoising, and chimera removal, 921,039 contiguous reads were retained (81% retention). There were between 62,893 and 89,745 reads per sample with an average read length of 307 bp. Samples were rarefied to 62,893 reads. After clustering amplicon sequence variants at 97% identity and removing singletons, there were 220 OTUs with rarefaction curves indicating saturation and each sample containing between 19 and 51 OTUs (Figure 10). Copepod sequences comprised 92% of sequences and were made up of 90 OTUs. All remaining non-copepod contaminant sequences (8%) were removed and excluded from downstream analyses. 98.6% of copepod sequences were identified to species with 12 species (15 OTUs) making up 93.3% of copepod sequences (Figure 11B).

Small copepod species comprised a significant portion of the naupliar community. These taxa included three cyclopoids (*Oithona similis*, *Oithona atlantica*[1], and *T. borealis*) and three calanoid species (*Pseudocalanus mimus*, *Pseudocalanus minutus*, and *Pseudocalanus newmani*). Collectively, the small copepods comprised two thirds of total naupliar cohort sequences with reads relatively evenly distributed across the six species (Figure 11B). Large copepod species comprised a quarter of total naupliar cohort sequences. Large species were present in similar ratios when compared with the bulk community samples (Figure 11A) with *N.*

flemingeri, *M. pacifica*, and *A. longiremis* comprising the majority of large copepod sequences. *Calanus marshallae, M. okhotensis, and N. plumchrus* made up a smaller fraction of sequences. Other species, including *Paraeuchaeta elongata*, *Lucicutia flavicornis*, and *Epilabidocera longipedata*, not consistently present in bulk community and naupliar cohort samples are not discussed further.

8.3.2 Individual sample composition

Species composition of small-size-fraction bulk community (Figure 12) and naupliar cohort samples (Figure 13) varied over time and depth, indicating both spatial and temporal differences in naupliar communities. Many species displayed affinity for a particular depth stratum (*T. borealis, O. atlantica*[1]*, P. mimus, A. longiremis*, *N. plumchrus* and *M. pacifica*) while others were present across all three depth strata (*N. flemingeri*, *P. minutus*, and *O. similis*). *Triconia borealis* and *N. plumchrus* were primarily in the 200-280 m depth stratum while *O. atlantica*[1], *A. longiremis*, and *M. pacifica* made up a larger fraction of upper water column reads. Sequence data demonstrate a seasonal progression in species presence with some species being more prevalent earlier in the sampling period and other species being more prevalent later in the sampling period. Shifts in community composition and species-specific recruitment patterns are explored in greater detail below.

The contribution of large copepod reads to the small-size-fraction bulk community sample reads varied over time and depth, ranging from 2% to 30% of total sample reads (Figure 12). The three dominant large copepod species, *N. flemingeri*, *M. pacifica*, and *A. longiremis* differed in their vertical and temporal distributions. Prior to February 7th, *N. flemingeri* was the dominant large-copepod species, making up between 5-18% of total sample reads in all three depth strata. Their relative number of reads declined over time and was nearly absent (<0.2%) by March 24th. *Metridia pacifica* was consistently present, ranging between 2% and 10% of reads,

in the 0-100 m and 100-200 m depth strata during the whole sample period. *Acartia longiremis* was primarily present in the upper 100 m in the latter portion of the sampling time period with sequences were nearly absent in January but increased later reaching a maximum of 7.8% of reads on March 24th in the 0-100 m samples. *Neocalanus plumchrus, M. okhotensis*, and *C. marshallae* made up no more than 1.8%, 3.6%, and 0.6% in any small size fraction sample, respectively. Overall, *N. plumchrus* was primarily present before March in the 200-280 m stratum whereas *M. okhotensis* and *C. marshallae* were primarily present on March 24th.

The medium size fraction bulk community samples captured the prevalence of copepodite stages (Table 2). Overall, large copepods made up the largest proportion of sequences at the surface (Figure 12). The relative reads for *N. flemingeri*, *M. pacifica*, and *M. okhotensis* increased over time from February to March. *Acartia longiremis* sequences initially declined until late February but increased again on March 24th. *Paraeuchaeta elongata* was uniquely found in the 200-280 m depth stratum medium size fraction samples.

Small copepod species made up a significant portion of all naupliar cohort samples, comprising between 38% and 85% of sample reads (Figure 13). The large copepod taxa displayed similar patterns in relative read abundance as described above. As with the large species, small species patterns differed over time and vertical space. *Oithona atlantica*[1] made up the largest fraction of sequences (~50%) in December and January 0-100 m samples but declined over time. *Oithona similis* (4%- 39%) and *T. borealis* did not have clear temporal patterns, however *T. borealis* made up a larger proportion of 200-280 m samples (36-76%) compared to other depth strata. All three *Pseudocalanus* species were present on, or before, January 5th and increased in their relative contribution to sequences later in the sampling period.

8.4 COMMUNITY ANALYSIS

A two-dimensional nMDS analysis on naupliar cohort data (n = 12, stress = 0.099) showed both temporal and vertical differences in community composition (Figure 14). Vectors of environmental parameters and community diversity metrics were fit along the direction of steepest increase in two-dimensional space. Temporal differences, represented by the day of year (DOY), were most strongly correlated with community composition (R^2 = 0.9135, p = 0.004). This indicates a strong seasonal progression of the naupliar community between the winter and spring. Significant correlations with *in-situ* fluorescence (R^2 = 0.8469, p = 0.010) and temperature (R^2 = 0.6578, p = 0.036) further support a shift in community structure correlated with the seasonal increase in phytoplankton and decrease in surface temperatures between winter and spring. Salinity was most strongly associated with the depth and there was a significant correlation (R^2 = 0.8112, p = 0.010) in naupliar community composition across depth strata. Community diversity, as measured by species richness (represented by number of copepod species), was highest in surface samples and later in the sampling period (R^2 = 0.7584, p = 0.017) and was strongly associated with increasing fluorescence. This is consistent with expected increases in naupliar recruitment associated with bloom-fueled reproduction at the surface. Simpson diversity and Pielou's evenness indices were not significantly correlated with the nMDS ordination (p = 0.076 and p = 0.162, respectively).

8.5 NAUPLIAR PHENOLOGY

Hierarchical cluster analysis on Wisconsin-double-standardized sequence counts was used to group individual species by their seasonal naupliar phenology (Figure 15). Nauplii from 6 species present in the 53-210 µm bulk community and 12 species present in the naupliar cohort metabarcoding samples sorted into three clusters representing three phenological strategies (Figure 16). Naupliar reads in group 1 (G1), which included *N. flemingeri*, *N. plumchrus*, and *O.*

atlantica[1], were most abundant early in the sampling period and declined over time. This contrasts with group 2 (G2) containing *C. marshallae*, *M. okhotensis*, and *A. longiremis*, which were nearly absent in January and February but present starting in March. Interestingly, species in group 3 (G3) showed an intermediate pattern; nauplii from species within this group were present throughout the sampling period with an increase in relative read abundance between the end of February and end of March. Species in G3 included *M. pacifica, P. minutus, P. mimus*, *P. newmani, O. similis,* and *T. borealis*.

Scatterplots of integrated chlorophyll α and the Wisconsin-double-standardized relative abundances revealed contrasting patterns for the three groups. G1 had a negative relationship and G2 and G3 had a positive relationship to integrated chlorophyll α measurements between December and March (Figure 17). For G1, individual species' reads were highest when chlorophyll α was low. In contrast, the percentage of G2 and G3 species reads increased as chlorophyll α increased. The difference between G2 and G3 was that G2 was absent when integrated chlorophyll α values were less than 5 mg/m^2 whereas G3 species were still present, although in lower proportions.

8.6 OVIGEROUS FEMALES

On January 5th, the presence of ovigerous or egg-bearing females were clearly distinguishable for three copepod species (Figure 18). These included *N. flemingeri*, *C. marshallae*, and *O. similis*, for which 69%, 2%, and 1% of the species' total population were ovigerous, respectively. Nevertheless, the small percentages for *C. marshallae* and *O. similis* still translated into relatively high numbers of ovigerous females given their overall high abundances (Figure 6). Despite the naupliar presence of *O. spinirostris*[1], *M. pacifica*, *Pseudocalanus* spp., and *T. borealis* on January 5th*,* no ovigerous females were observed, suggesting a mismatch between naupliar presence and the observation of reproductively active females.

As time progressed, the number of species and the percentage of ovigerous females increased. All species except *N. flemingeri* and *O. spinirostris*[1] were reproductively active on March 24th and continued into April for *C. marshallae, Pseudocalanus,* and *O. similis. Triconia borealis* and diel-vertical-migrating *Metridia* are primarily present at depth. Therefore, the absence of reproductive females for those two species in April may be a sampling artifact since no collections were made below 100 m.

9 DISCUSSION

The aim of this study was to characterize the species-specific naupliar recruitment patterns for copepods in the Northern Gulf of Alaska during the winter-to-spring transition. Environmental changes observed over the duration of the sampling period were consistent with previously described seasonal patterns of decreasing surface temperature, increasing surface salinity, stable conditions below the sill depth, and increasing surface chlorophyll leading to the spring bloom (Heggie et al., 1977; Stabeno et al., 2004). Low zooplankton abundances in the surface waters during the winter contrasted with the unexpectedly diverse and abundant overwintering copepod community concentrated in the deep depth stratum. Abundances at depth were comparable to those in the upper 100 m during the spring bloom (Cooney et al., 2001; Coyle and Pinchuk, 2003). Nauplii were found at all depths and timepoints. The wintertime nauplius population was comprised of a diverse assemblage of species with a changing community composition from late December to early May.

Species-specific naupliar recruitment phenologies clustered into three groups: bloom-independent (G1), bloom-dependent (G2), and semi-bloom-dependent (G3). The observed phenologies align remarkably well with patterns outlined by Heinrich (1962), which were based on limited species-specific life history data and not substantiated by winter sampling. This study used an integrated approach to categorize copepod species by their phenological pattern in

Resurrection Bay. Naupliar presence and absence was contextualized with observed copepod abundances, stage distributions, and presence of ovigerous females. Below, case studies of the species-specific naupliar recruitment patterns are discussed in greater detail.

9.1 BLOOM-INDEPENDENT SPECIES (G1)

The bloom-independent group consisted of two capital-breeding *Neocalanus* species and one income-breeding species of *Oithona*. Metabarcoding results indicated naupliar presence for all three species was highest in the winter, between December and February, when total naupliar abundances were relatively high (> 1000 individuals/m^3) but chlorophyll concentrations were low (Figure 7, 15 & 17). As the season progressed, the relative read abundances of G1 species declined and comprised a very small proportion of the samples starting in late March, even though naupliar abundances increased. While the early presence of the capital-breeding *Neocalanus* was expected based on their ability to utilize lipid reserves to fuel reproduction (Lenz and Roncalli, 2019), the pattern was not expected for *Oithona.*

9.1.1 *Neocalanus* spp.

Nauplii of *N. flemingeri* were observed in DNA metabarcoding samples in December and January. The timing of naupliar presence coincided with the presence of ovigerous females. By February 22nd, no female *N. flemingeri* were recorded, indicating the termination of the reproductive period (Figure 9). Nauplii disappeared at the same time, first from the 200-280 m depth stratum on February 22nd and then the entire water column by the end of March. As the presence of naupliar sequences declined, there was an increase in relative reads in the medium-size-fraction bulk community metabarcoding samples and CI and CIIs appeared in the upper 100 m in late February and March. By April, the population included a large proportion of CIVs.

The early presence of nauplii alongside the presence of ovigerous females confirms that this species reproduces between December and the end of February in the Gulf of Alaska. The timing of reproduction in Resurrection Bay is also consistent with reported development times for *N. flemingeri* and the spring copepodite stage composition in the Gulf of Alaska (Cooney et al., 2001; Hopcroft and Clarke Hopcroft, 2019; Hopcroft, 2021; Liu and Hopcroft, 2006; Slater, 2004). Despite a more northern collection location, the phenology of *N. flemingeri* in Resurrection Bay is similar to that reported in the eastern North Pacific (Station P; 50°N, 145°W) and western Pacific (Site H; 41.5-42.5°N, 145-146°E) based on the timing of reproductively active females (Kobari and Ikeda, 2001; Miller and Clemons, 1988). This is also the first demonstration that *N. flemingeri* diapauses and reproduces in small fjord systems at shallower depths than previously reported.

Reproduction occurred at depth as females. *Neocalanus flemingeri* females were only found in the 200-280 m depth stratum, consistent with reports from other studies (Kobari and Ikeda, 2001; Miller and Clemons, 1988). However, *N. flemingeri* nauplii were found at all depths, including the 0-100 m depth stratum in December. The ontogenetic migration of the nauplii has been suggested based on the occurrence of copepodites in the upper 100 m in March (Miller and Clemons, 1988). However, this is the first report of the depth distribution of *N. flemingeri* nauplii, which suggests that migration to shallower depths occurs soon after hatching and before substantial increases in food resources. Early ontogenetic migration may reduce the risk of predation in the 200-280 m depth stratum given high abundances of predatory copepods (e.g. *Oithona spinirostris*, *Metridia* spp., and *Paraeuchaeta elongata*, this study), other zooplankton, as well as demersal fish predators (Landry and Fagerness, 1988; Mauchline, 1998; Mueter and Norcross, 2002).

The timing of naupliar development into copepodite stages coincided with the increase in phytoplankton around March 12th. This timing indicates that surviving nauplii that were spawned in December and January may have spent over 2 months in the naupliar stages. Thus, it is possible that nauplii enter dormancy and delay development in the NII and NIII stages until optimal food conditions arrive. There is some support for this hypothesis from laboratory studies on *N. flemingeri* nauplii and observations in the congener *N. plumchrus* (Fujioka et al., 2015; Roncalli et al., 2022; Saito and Tsuda, 2000; Slater, 2004). However, whether the nauplii undergo a period of dormancy in January and February will require further examination of their stage composition, physiology, and *in-situ* growth rates.

In addition to *N. flemingeri,* nauplii of *Neocalanus plumchrus* were present in both the small-size-fraction bulk community samples and naupliar cohort samples, albeit at low relative percentages (Figure 12 & Figure 13). Despite the low relative read abundance, hierarchical cluster analysis placed *N. plumchrus* with *N. flemingeri* based on their similar phenologies (Figure 15). Sequences were primarily found in the 200-280 m depth stratum between January and February and absent in March. Due to a lack of deeper sampling in December, any deep *N. plumchrus* nauplii present would have been missed. The deeper depth distribution of *N. plumchrus* aligns with the depth distribution of *N. plumchrus* nauplii in the Oyashio region (Fujioka et al., 2015), but contrasts with the observed early upward ontogenetic migration observed for *N. flemingeri*. Stage CV and female *N. plumchrus* were absent from samples, consistent with the species' more offshore distribution compared to *N. flemingeri* (Hopcroft and Clarke Hopcroft, 2019; Hopcroft, 2021).

The spring disappearance of *N. plumchrus* nauplii did not co-occur with the appearance of copepodites. Based on Fujioka et al. (2015), it was expected that *N. plumchrus* nauplii and early copepodites would be present in the upper 100 m in March and April. However, negligible *N.*

plumchrus sequences (< 0.2%) were found in the medium size fraction bulk community samples, raising a question about the fate of the nauplii. Below 200 m, *N. plumchrus* nauplii were likely exposed to high levels of predation due to the concentration of predatory copepods and other zooplankton below 200 m as well as close proximity to the benthos and demersal fish predators. It is possible that *N. plumchrus* nauplii in the shallower Resurrection Bay faced higher predation pressures in comparison to their offshore counterparts as well as upward-migrating *N. flemingeri* nauplii—leading to poor inshore survival of *N. plumchrus*.

9.1.2 Oithona spinirostris (*atlantica*)[1]

The third species in G1 was the large-bodied *Oithona spinirostris* (*atlantica*)[1]. Here, *O. spinirostris* (as identified in formalin samples) and *O. atlantica* (as identified in DNA metabarcoding samples with 100% identity) will be discussed synonymously. However, further taxonomic review[1] is required to properly identify the large-bodied *Oithona* in the Gulf of Alaska.

O. spinirostris (atlantica)[1] naupliar sequences were primarily present at the beginning of the season in the upper 100 m (Figure 13), making up approximately half of the reads on both December 28th and January 5th, during a period of minimum prey availability (Figures 3-5), coinciding with high abundances of cyclopoid nauplii (Figure 7). The proportion of reads then decreased in February following an overall decrease in cyclopoid naupliar abundance (Figure 7 & Figure 13). The proportion of reads remained low in March. While both *O. spinirostris (atlantica)[1]* and *Oithona similis* are income breeders, the two species displayed differing phenologies with an unexpected early occurrence of *O. spinirostris (atlantica)[1]* nauplii.

The *O. spinirostris (atlantica)[1]* population consisted of primarily juvenile copepodites with a small percentage of females. Egg-bearing females were only observed on February 22nd. This is the first of several cases where the data suggest a mismatch between the presence of nauplii and

an apparent absence of reproductive females, which is discussed in more detail below. Nevertheless, it should be noted that the ovigerous females observed in February preceded the March increase in chlorophyll α and later spring bloom. *O. spinirostris* females have been shown to consume copepod nauplii up to 500 µm with preferred prey length of 100 µm, as demonstrated in feeding experiments (Landry and Fagerness, 1988). A large portion of the naupliar population was near this 100 µm size range and potentially served as a prey source when phytoplankton, dinoflagellate, and ciliate biomass were still low (Figure 9, Figure 3, & Figure 5). Alternatively, *O. spinirostris (atlantica)*[1] may be more tolerant to low food conditions like it's congener, *O. similis* (Zamora-Terol et al., 2013).

9.2 BLOOM-DEPENDENT SPECIES (G2)

The bloom-dependent group, comprised of *Acartia longiremis*, *Metridia okhotensis*, and *Calanus marshallae*, was characterized by an absence of nauplii earlier in the winter during January and February followed by recruitment in March and April. While all three species were clustered together based on their later reproductive phenologies, the exact timing of naupliar presence differed among the species. Naupliar presence of the income-breeding *A. longiremis* and *M. okhotensis* coincided with a moderate increase in chlorophyll α during March prior to the main spring bloom, which began on April 20th in the Gulf of Alaska (Ballantine, 2024). Reproduction of *C. marshallae* was more closely tied to the spring bloom. Overall, these three species made up a small fraction of sequences in all bulk community and naupliar cohort samples (Figure 11).

9.2.1 Acartia longiremis

The first G2 species to appear as nauplii in the bulk community samples was *A. longiremis* with an absence of sequences in January and the initial recruitment of its nauplii observed on February 7th. Sequences were present in the upper 100 m and increased in relative proportion

over time (Figure 12). Development of the next generation of early copepodites was evident on March 24th with an increase in CI-CIV stages (Figure 9), coinciding with an increase in *A. longiremis* sequences in the medium size fraction on March 24th (Figure 12). This is consistent with observations of increasing *A. longiremis* copepodite abundances in the spring in Prince William Sound, Alaska (McKinstry and Campbell, 2018).

The January and February overwintering populations were predominately female (Figure 9). The presence of ovigerous females was not quantified for this study. The observed overwintering females is consistent with descriptions of overwintering diapausing females and absence of other stages in Norway (Norrbin, 1994). However, it contrasts with observations in the Baltic Sea where *A. longiremis* were observed to be present in all stages, including nauplii, throughout the winter and potentially maintaining low levels of winter reproduction (Peters et al., 2013).

The source of *A. longiremis* nauplii remains ambiguous. Most *Acartia* produce resting eggs and *A. longiremis* have been hatched from egg deposits in sediments off northern California (Baumgartner and Tarrant, 2017; Marcus, 1990). However, in Balsfjorden, Norway, diapausing females have been described to utilize lipid reserves for gonadal maturation and potentially fuel the production of the first clutch of eggs in early spring (Norrbin, 2001, 1996, 1994). The appearance of *A. longiremis* naupliar sequences on February 7th is prior to the moderate March 12th bloom and eventual spring peak in productivity (Figures 3-5). This raises the possibility that *A. longiremis* exhibits a hybrid strategy using lipids to fuel their first clutch of eggs when phytoplankton availability is low and then switch to income breeding during the spring and summer. However, the results do not preclude the possibility of naupliar recruitment from sediment egg banks. Further work, such as sediment incubations, is required to better understand the reproductive strategy of *A. longiremis* in the Gulf of Alaska.

9.2.2 Metridia okhotensis

The second G2 species to appear as nauplii was *M. okhotensis*. Sequences were absent in December and January samples (Figure 12 & Figure 13). They comprised a small fraction of sequences in the February samples with a larger contribution on March 24th at all depths in the bulk community samples. This aligns with observations of spring egg production in both the Northern Gulf of Alaska and the Oyashio region for *M. okhotensis* (Arima et al., 2016; Hopcroft et al., 2005). The absence of *M. okhotensis* sequences in April and May was unexpected. Overall, *M. okhotensis* sequences were rare in naupliar cohort samples, likely due to the smaller sample size of nauplii compared to bulk community samples. Therefore *M. okhotensis* could have been missed in the April and May samples which were only analyzed via the naupliar cohort method. Nauplii of *M. okhotensis* started to develop into copepodites in March, as indicated by an increase in sequences in the medium size fraction bulk community samples after March 12th and presence of CI-CIII stages by March 24th (Figure 9 & Figure 12).

Overwintering *M. okhotensis* were in the CV stage on January 5th, which is consistent with an absence of females observed after October by Hopcroft and colleagues (Figure 9) (Hopcroft et al., 2005). By February 22nd, approximately two-thirds of the CV population transitioned into adult male and female stages with a small percentage being ovigerous. The highest percentage of ovigerous females occurred on March 24th, corresponding to the increase in naupliar recruitment (Figure 18). The increase in ovigerous females coincided with the small increase in phytoplankton during March. As a strong diel-vertical-migrator, female *M. okhotensis* were not collected during the day in the April 22nd 0-100 m sample (Takahashi et al., 2009).

9.2.3 Calanus marshallae

C. marshallae had the latest reproductive phenology of the G2 species and was most closely tied to the spring bloom. Naupliar sequences were first present on March 24th above 200 m

(Figure 13). The fraction of *C. marshallae* sequences increased in the 0-100 m depth stratum on April 22nd but were absent in May. This absence in May was likely a result of overall low abundance and small sample size in the naupliar cohort design. The majority of *C. marshallae* copepods were in the CV stage on both January 5th and February 22nd (Figure 9). It wasn't until March 24th that a significant portion of the population developed into adult female stages, which were primarily non-ovigerous. The proportion of ovigerous females increased in April and coincides with the spring increase in *C. marshallae* naupliar sequences (Figure 18). The development of the next generation of early copepodites was not observed for *C. marshallae* (Figure 9).

Based on the lack of naupliar presence prior to March and later development of females, the phenology of *C. marshallae* appears to be more like that of the income-breeding populations off the Oregon coast (Peterson, 1979). This contrasts with *C. marshallae* populations described in the Bering Sea, for which a large fraction of the population was ovigerous by February and egg production occurred prior to the spring bloom likely fueled by lipid reserves (Baier and Napp, 2003). Therefore, it appears that *C. marshallae* life history and reproductive strategies vary latitudinally, like *Calanus finmarchicus,* with the more southern populations exhibiting later reproduction and greater reliance on spring phytoplankton to fuel reproduction (Hirche, 1996).

A small fraction of C*. marshallae* sequences were also present between January and February in the 200-280 m depth stratum (Figure 12). While the small proportion of ovigerous females present in January could explain this, body fragments of larger copepods were often present in the small size fraction (Figure 18). This was particularly common in the 200-280 m depth stratum where copepod abundances were highest. Given the high biomass of *C. marshallae* copepodites in the 200-280 m depth stratum early in the season, contamination from copepod fragments is probable and could explain the small fraction of *C. marshallae* reads observed

below 200-280 m (Figure 6). This inference is supported by a lack of *C. marshallae* sequences in the corresponding naupliar cohort samples during January and February.

Despite the initially high biomass of its copepodites, *C. marshallae* made up a very small proportion of bulk community and naupliar cohort sequences (Figure 6 & Figure 11). A nearly ten-fold decline in *C. marshallae* biomass was observed between January and March (Figure 6 & Figure 8). Like *N. plumchrus*, which has been reported to experience significant winter mortality of diapausing copepodites due to predation, diapausing *C. marshallae* copepodites could have experience high levels of predation especially due to their occurrence at depth and proximity to benthic predators (Mackas and Tsuda, 1999; Mueter and Norcross, 2002).

9.3 SEMI-BLOOM-DEPENDENT SPECIES (G3)

The semi-bloom-dependent group was comprised of four calanoid species (*Metridia pacifica*, *Pseudocalanus mimus*, *Pseudocalanus minutus*, and *Pseudocalanus newmani*) and two cyclopoid species (*O. similis and Triconia borealis*) (Figure 15). Despite being considered income-breeding species, naupliar sequences of the six species were present in considerable proportions during late December and early January when prey availability was at a minimum (Castellani et al., 2007; Hopcroft et al., 2005; Mauchline, 1998; Napp et al., 2005). In contrast to the three species in G1, the proportion of sequences attributed to G2 species increased over time. For all G3 species except *O. similis*, there was a mismatch between the timing of nauplii and ovigerous females with nauplii occurring earlier than the presence of ovigerous females.

9.3.1 *Metridia pacifica*

Metridia pacifica sequences were present consistently in the small-size-fraction bulk community samples and naupliar cohort samples throughout the entire sampling period from December to May, especially in the upper 200 m (Figure 12 & Figure 13). The percentage of *M. pacifica*

reads stayed mostly constant over time. These results contrast with observations at Station P, which showed a steep decline in *M. pacifica* naupliar abundances starting in November and their absence in January (Batchelder, 1985). Instead, it more closely aligns with observations from Funka Bay, Japan, which described continual *M. pacifica* naupliar presence between January and March (Nakatani, 1995).

Despite naupliar presence early in the sampling season, ovigerous *M. pacifica* females were not observed on the January 5th or February 22nd timepoints (Figure 18). The January 5th overwintering population consisted of primarily males, CVs, and non-ovigerous females (Figure 9). Ovigerous females were not observed until March 24th. This is nearly three months after the first observation of naupliar sequences in December. Therefore, despite the potential for *M. pacifica* to switch to a more omnivorous diet (Wong, 1988), reproduction still appears to be closely linked to phytoplankton availability based on winter stage distribution and lack of ovigerous females. While northern Gulf of Alaska *M. pacifica* females have been shown to produce eggs in December and March, eggs did not develop normally until April and May when egg production rates peaked associated with the spring bloom (Hopcroft et al., 2005). The observed winter presence of nauplii is independent of reproductive activity or spring phytoplankton production. This leads to the hypothesis that a portion of the *M. pacifica* population overwinters as nauplii. However, it may also be possible that nauplii could have been advected from reproductive populations outside of Resurrection Bay or ovigerous females were present but missed in the samples.

The proportion of next-generation CI and CII recruits gradually increased between January and March (Figure 9). This was matched by an increase in the proportion of *M. pacifica* sequences in the medium size fraction samples particularly at the end of February and March (Figure 12).

The cooccurrence of several stages, including nauplii, and continual increase of early copepodite stages indicates *M. pacifica* might exhibit an asynchronous life-history strategy.

9.3.2 *Pseudocalanus* spp.

Naupliar sequences of the three co-occurring *P. minutus, P. mimus*, and *P. newmani* were present in naupliar cohort samples. Collectively, the three species made up approximately one quarter of the total reads (Figure 11). *Pseudocalanus* spp. is a complex of several species with *P. minutus, P. mimus,* and *P. newmani* being the three dominant species in the Northern Gulf of Alaska (Napp et al., 2005). Species-specific life histories are not well known for *Pseudocalanus* spp. since naupliar and copepodite stages are difficult to distinguish morphologically. Instead, the species are most easily separated using molecular approaches (Bucklin et al., 2001; Ershova et al., 2017). This study's use of DNA metabarcoding techniques allowed for a better characterization of the three species' life histories in the Gulf of Alaska.

All three species were placed in G3 based on their similar naupliar phenology. *Pseudocalanus* sequences were present early in the sampling period between late December and early January and increased in relative composition over time. The maximum percentage of *Pseudocalanus* sequences occurred on March 24th in the 0-100 m sample, collectively making up nearly two-thirds of the DNA sequences. Afterwards, the total relative reads of the three species remained high in April and May. This coincided with an overall increase in naupliar abundances, further supporting an increase in *Pseudocalanus* naupliar abundances (Figure 7). The pattern in Resurrection Bay is similar to the one reported in Funka Bay, Japan (Nakatani, 1995). A ten-fold increase in the proportion of CI *Pseudocalanus*, which couldn't be distinguished to species, was observed between February 22nd and March 24th, similar to observations in the Bering Sea of increasing development of early copepodites during the spring (Vidal and Smith, 1986).

The largest proportion of *Pseudocalanus* sequences were identified as *P. minutus* (16%)—a species that tends to be abundant in fjord systems like Prince William Sound as opposed to the open Gulf of Alaska (Napp et al., 2005). Nauplii of *P. minutus* were distributed across all depth strata (Figure 11). Like *M. pacifica*, there was a mismatch between the winter presence of nauplii and later development of egg-bearing females. On January 5th, the population primarily consisted of unidentified *Pseudocalanus* CIV and CV stages with very few females with none being egg-bearing. By February, there were fewer copepodites while the percentage of adults, including egg-bearing females, increased. *Pseudocalanus minutus* was the only *Pseudocalanus* species with egg-bearing females in February.

Pseudocalanus mimus and *P. newmani* differed in their vertical distribution and timing of reproductive females compared to *P. minutus*. The two species each comprised approximately 5% of naupliar cohort and were primarily observed in the 0-100 m depth stratum (Figure 13). Similar to *P. minutus,* there was a mismatch between nauplii and reproductive females. However, the duration of mismatch between nauplii and reproductive females was even greater for these two species. Egg-bearing females were not observed until March and increased in abundance in April, which is consistent with egg production rates for these two species reaching a peak in May (Napp et al., 2005).

9.3.3 *Triconia borealis*

Triconia borealis was the only oncaeid copepod species identified in the metabarcoding samples. Sequences were consistently present throughout the sampling period and made up a large fraction of the 200-280 m naupliar cohort samples (Figure 13). This aligns with high abundances of cyclopoid nauplii located below 200 m (Figure 7). *Triconia borealis* sequences were less prevalent above 200 m and thus not observed in the December, April, and May samples that were only collected in the 0-100 m depth stratum (Figure 15). Adult *T. borealis* in

the western subarctic Pacific migrate deeper during the late winter (Nishibe and Ikeda, 2006), which is consistent with the deeper depth distribution of observed adults and copepodites in Resurrection Bay. However, the depth distribution of the nauplii has not been previously described.

The early presence of *T. borealis* nauplii contrasts with the expected spring reproduction based on studies in the Oyashio region where egg-bearing *T. borealis* were present in May and June but absent between December and March (Nishibe and Ikeda, 2006). However, the presence of nauplii in Resurrection Bay occurred prior to egg-bearing *T. borealis,* which were not observed until late March. Instead, the majority of *T. borealis* were juvenile copepodites. Because winter nauplii were primarily present in isolated waters below the fjord sill (Heggie and Burrell, 1981), the earlier presence of nauplii without apparent reproductive females is unlikely explained by advection of nauplii from outside reproductive females and could indicate the presence of overwintering nauplii. As a detritivore, deep *T. borealis* could feed on exported particulate organic matter, such as *Neocalanus* carcasses, and resuspended sediments to fuel winter reproduction (Steinberg and Landry, 2017; Yamaguchi et al., 2002). Yet despite the likely availability of non-phytoplankton food resources in the winter, the appearance of egg-bearing *T. borealis* still coincided with a period of increased vertical export of diatoms, suggesting the importance of phytoplankton prey for fueling the species' maturation and reproduction (Figure 5).

9.3.4 *Oithona similis*

Nauplii of one species, *O. similis,* cooccurred with egg-bearing females. Naupliar cohort samples indicate that *O. similis* nauplii were present consistently between late December and May with no clear depth preference (Figure 13). In addition, egg-bearing *O. similis* were present at all timepoints, making *O. similis* the only G3 member without an apparent mismatch between

naupliar presence and ovigerous females. Maintenance of low-level winter reproduction has been reported for *O. similis* in sub-Arctic and Arctic waters (Balazy et al., 2021; Dvoretsky and Dvoretsky, 2009; Lischka and Hagen, 2005; Zamora-Terol et al., 2013). Furthermore, females off the coast of Greenland were actively feeding during the winter, in spite of low prey field concentrations including chlorophyll α concentrations and diatom, dinoflagellate, and ciliate biomass that were similar to those found in Resurrection Bay (Zamora-Terol et al., 2013). Moreover, Zamora-Terol and co-authors found that the reproductive efficiencies for the females was higher during the winter than the spring (Zamora-Terol et al., 2013).

The proportion of egg-bearing females increased over time as chlorophyll concentrations increased. This was matched with a relative increase in the percentage *O. similis* naupliar sequences over time and overall increase in cyclopoid abundances, which is consistent with previous descriptions of increased egg production during the spring leading to an eventual peak in reproduction and abundances in the summer (Castellani et al., 2007; Coyle and Pinchuk, 2003; Dvoretsky and Dvoretsky, 2009; Lischka and Hagen, 2005).

9.4 INTERPRETATION OF METABARCODING DATA

It is important to use caution when interpreting metabarcoding data. Relative read composition cannot be interpreted directly as absolute abundance or biomass for several reasons. While relative read composition has been shown to be significantly correlated with biomass, correlations are often weak and vary across taxonomic groups (Ershova et al., 2021). Sources of bias include differences in biomass:DNA copy ratios, differential DNA extraction success between species, different PCR amplification rates, variability in sequencing, and selection of bioinformatic pipelines (Lamb et al., 2019). Copepods have been shown to have stronger correlations with biomass using the Leray mCOI primers in comparison to other taxa (Matthews

et al., 2021). Because this study is focused on copepod nauplii, these primers were selected to reduce biases in extraction success and amplification, especially in the naupliar cohort samples.

Moreover, as a relative index, percentages of sequences cannot be interpreted as absolute numbers as they are impacted by the total community biomass. For example, one might interpret a decline in a species' relative reads as an overall decline in biomass. However, if the total community biomass increases, as it occurred between February and March, the species could experience an overall increase in absolute biomass while comprising a smaller proportion of the total biomass. If the direction of change is the same (i.e. an increase in sequences alongside an increase in biomass), one can more reliably interpret the overall direction (but not magnitude) of change.

The increase in relative reads for the species in G2 and G3 groups between January and March are matched by an overall increase in naupliar biomass. Therefore, the increase in relative reads is likely to reflect an overall increase in naupliar biomass for these species. In contrast, the overall decline in naupliar biomass between January 5th and February 22nd suggests that increases in relative numbers of reads may not represent increases in biomass. However, the decline in relative read abundance for *Neocalanus* can be interpreted as a real decrease in biomass especially given the absence of reads in both bulk community and naupliar cohort samples starting March 24th despite an overall increase in naupliar biomass.

Differences in relative read abundances of large-bodied copepods between bulk community and naupliar cohort samples could be attributed to several of sources. First, by extracting DNA from only 100 nauplii, naupliar cohort samples processed a smaller sample size of the naupliar community and are therefore less likely to capture rare taxa (< 5% contribution to reads). This is relevant for species with low but consistent presence in bulk community samples but patchy

presence in naupliar cohort samples, such as *A. longiremis* and *M. okhotensis*. Second, body fragments like antennule pieces of larger copepods were often present in the 53-210 µm size fraction in bulk community samples. This was particularly true in the 200-280 m depth stratum where copepod abundances were highest. The presence of non-naupliar tissue could result in small amounts of contamination and lead to a signal where a species is present in the bulk community samples but not in the naupliar cohort samples.

9.5 INCOME AND CAPITAL BREEDING STRATEGIES

It was hypothesized that the presence of nauplii would be dictated by a species' income or capital breeding strategy. Capital- and hybrid-breeding species were expected to be present earlier in the season due to their lack of reliance on the spring bloom. Income-breeding species were not expected to be present until later when prey availability was sufficient to fuel reproduction (Jönsson, 1997; Sainmont et al., 2014; Varpe et al., 2009). Cluster analysis separated the capital breeding species (G1) from the income breeding species (G2 and G3) based on naupliar phenologies.

For the capital-breeding G1 members, *N. flemingeri* and *N. plumchrus,* nauplii were present during the winter coinciding with a minimum in prey abundances. The decoupling of reproduction from food availability has been hypothesized to increase species fitness by allowing nauplii to develop during a period when predation risk is lower and allowing copepodites to be present during peak primary production (Varpe et al., 2009). For *Neocalanus*, reproduction during the winter positions the lipid-accumulation CV phase during the height of the spring bloom, maximizing their ability store capital for the following year (Lenz and Roncalli, 2019; Roncalli et al., 2023). The early production of *N. flemingeri* nauplii enabled the appearance of early copepodite stages in March with later copepodite stages present during the spring bloom in April.

The later recruitment of G2 nauplii was consistent with the income-breeding strategy requiring food prior to reproduction. While *C. marshallae* has been described as both a hybrid and income breeder in different regions (Baier and Napp, 2003; Peterson, 1979; Vidal and Smith, 1986), in Resurrection Bay it behaves like an income breeder. The direct conversion of feeding to reproductive output is more efficient (Jönsson, 1997). Interestingly, the presence of ovigerous females and nauplii for *M. okhotensis* and *A. longiremis* occurred prior to the main spring bloom that started in April with early copepodites developing by the end of March. This suggests that adequate prey resources to fuel reproduction were available prior to the spring bloom for these two species.

The winter presence of G3 nauplii (plus G1 *O. spinirostris* (*atlantica*)[1]) was unexpected given their income-breeding strategies. For all species except *O. similis*, ovigerous and egg-bearing females were not observed in January despite having naupliar presence. Ovigerous females were not observed until late February or March and suggests that egg production was tied to the increase in phytoplankton. While it is possible that reproductive females were missed in sample analysis or nauplii were advected into Resurrection Bay from reproductive populations elsewhere, the mismatch raises the question of whether overwintering naupliar stages may be more common than expected. Overwintering of marine copepod nauplii has only been described for the ice-associated Antarctic species, *Stephos longipes* and *Paralabidocera antarctica* (Atkinson, 1998). However, there is some evidence for a naupliar dormancy in *Neocalanus* spp. (Fujioka et al., 2015; Roncalli et al., 2022). Future sampling with greater spatial coverage would be required to verify if the absence of reproductive females is consistent throughout the Gulf of Alaska. Additionally, sediment incubations could be used to assess if *A. longiremis* nauplii hatch from diapausing egg deposits without the presence of reproductive females, as reported from the coast of California (Marcus, 1990).

The three-fold increase in chlorophyll in March, while still low (<1 µg/L), corresponded with the timing of new egg production of income breeding females (G2 & G3) prior to the main spring bloom. Ovigerous females were present for all income-breeding taxa on, or before, March 24th. Likewise, naupliar abundances tripled between February 22nd and March 24th, indicating significant naupliar recruitment of several income-breeding species prior to the April bloom. In April, naupliar abundances were lower despite the significantly higher chlorophyll concentrations. This raises the question whether peak naupliar recruitment precedes the spring bloom and was fueled by smaller increases in chlorophyll.

The moderate March increase in chlorophyll also appeared to have a significant impact on the development of both preexisting (G1 and G3) and newly produced (G2 and G3) nauplii. An increase in calanoid naupliar lengths between February and March coincided with the March increase in chlorophyll and the presence of larger, late-stage nauplii and the appearance of early copepodite stages. A notable increase in CI and CII copepodite stages on March 24th occurred for almost all calanoid species. This meant that a significant percentage of each species' population entered the main spring bloom as a next generation copepodite.

9.6 BROADER IMPLICATIONS

The copepod community present in Resurrection Bay is similar to communities in other fjord systems like Prince William Sound and the greater Gulf of Alaska (Cooney et al., 2001; Coyle and Pinchuk, 2005, 2003; Hopcroft et al., 2005; Napp et al., 2005; Paul et al., 1991). While there are notable exceptions, like *M. okhotensis* and *P. minutus* that are considered glacial relicts, the results from Resurrection Bay provide insights into the life histories of copepods in the Gulf of Alaska more generally. Thus, the high abundances of overwintering and reproductive copepod populations within Resurrection Bay, particularly below the sill depth, may be a phenomenon

that occurs broadly in areas where bottom depths exceed 200 m. This study illustrates the ecological significance of deep-water habitat for diapausing *Neocalanus* and *Calanus*, as well as many other overwintering copepod species. Coastal areas and fjords like Resurrection Bay may be important refuges for overwintering copepods and sources of naupliar production during the winter-to-spring transition. It is well known that fjords, distributed along the previously glaciated coastlines of Alaska and British Columbia, provide important overwintering, breeding, and feeding grounds for ecologically and economically important fish and marine mammal species (Etherington et al., 2007; Paul et al., 1991; Renner et al., 2012). The spatial overlap of these predators with dense spawning populations of copepods could provide important feeding habitat for the upper trophic levels.

Several closely related species differed in their phenologies and were clustered in separate species groupings. Pairs of species included *N. flemingeri* (G1) and *C. marshallae* (G2), *M. okhotensis* (G2) and *M. pacifica* (G3), and *O. spinirostris (atlantica)*[1] (G1) and *O. similis* (G3). Such patterns serve as examples of temporal niche partitioning, by which taxa in competition for similar habitat or food resources shift their phenology to reduce overlap and interspecific competition (Hutchinson, 1961; Schoener, 1974). The differentiation of niches among species that perform similar ecological functions (functionally redundant species) leads to differing responses to environmental changes among the species and confers greater stability to an ecosystem (Biggs et al., 2020; Lindegren et al., 2016; Loreau and De Mazancourt, 2008; Tilman, 1996). This is known as the portfolio effect (Figge, 2004; Schindler et al., 2015). *Neocalanus* and *Calanus* are often grouped in analyses due to similarities in size, lipid, and diapause strategies (Arimitsu et al., 2021; Conover, 1988; Record et al., 2018), suggesting functional redundancy as defined by Biggs and coauthors (2020). Likewise, there are many ecological similarities between the congeners of *Metridia* (Hattori, 1989; Hopcroft et al., 2005; Takahashi et al., 2009) and *Oithona* (Hwang et al., 2010; Takahashi and Uchiyama, 2007). The

differing winter phenologies among these seemingly functionally redundant species provide an example of the portfolio effect among Northern Gulf of Alaska copepod species, potentially contributing to the overall stability of the Northern Gulf of Alaska ecosystem.

The characterization of the winter copepod community leads to a better understanding of the food web during a period of low primary production. Copepod nauplii are an important prey item for larval fish (Doyle et al., 2019). Larvae of many ecologically and economically important fish are present between January and March, including Walleye Pollock (*Gadus chalcogrammus*), Pacific Cod (*Gadus macrocephalus*), Pacific Halibut (*Hipoglossus stenolepis*), and Arrowtooth Flounder (*Atheresthes stomias*), and the winter-spring zooplankton prey availability, especially of nauplii, has been proposed as an indicator of larval fish survival (Doyle et al., 2019). The winter presence of *Neocalanus* nauplii, in particular, was hypothesized to be of large importance for winter-spawned larval fish based on the assumption that other nauplii would not be present (Doyle and Mier, 2016). However, this study found an abundance of other copepod species' nauplii during the winter, expanding the potential sources of prey availability. Moreover, phenological shifts in fish spawning have been documented for several species, including the earlier spawning of Walleye Pollock in the Gulf of Alaska (Alix et al., 2020; Rogers and Dougherty, 2019). While this may lead to changes in the prey field for larval fish, these data suggest that there will be overlap between the fish predators and copepod nauplii but may be of a different species. Thus, effects on the predator may not be a result of presence or absence of naupliar prey, but potentially differences in prey quality, emphasizing the importance of characterizing the winter naupliar prey availability for fish survival.

In summary, the copepod community in the winter is diverse and dynamic. Without the knowledge of who is present in the winter, it is difficult understand how changes in environmental conditions during the winter and climatic variability might impact the zooplankton

community structure and ecosystem in the spring. It has been hypothesized that environmental fluctuations, like the Pacific Decadal Oscillation (PDO) phase, affect spring copepod community composition (Kimmel and Duffy-Anderson, 2020). Describing the winter copepod community is the first step to better understanding the mechanisms by which winter environmental fluctuations, such as PDO, might influence spring zooplankton communities.

10 TABLES

Table 1. Summary table of processed samples from RES2.5 in Resurrection Bay, Alaska between December 28th, 2022, and May 4th, 2023. The core sampling period (January 5th to March 24th) is outlined with a thick line with supplemental samples collected outside the core period. Collection depths, size fractions (SF) where applicable, and expected total number of samples collected per collection date for each sample type are noted. Shaded cells indicate samples collected, processed, and discussed herein. Unless marked by an asterisk, gray cells represent the expected sample size. * = loss of one or more samples. ** = only 0-100 m samples were collected. Total number of samples (N) are tallied.

	Sample Type	Dec 28	Jan 05	Jan 20	Jan 27	Feb 07	Feb 22	Mar 12	Mar 24	Apr 22	May 04	N
Environmental	**CTD (n = 1/day)** (0-280 m)											7
	Chlorophyll a (n = 12/day) (0, 10, 20, 30, 40, 50 m; SF: < 20 & > 20 µm)	*		*								98
	Flow cytometry (n = 8/day) (0, 10, 20, 30, 40, 50, 150, 280 m)					*						39
	Microzooplankton (n = 3/day) (50, 150, 280 m)							*				11
Zooplankton	**Formalin (n = 3/day)** (0-100, 100-200, 200-280 m)									**		10
	Bulk Community (n = 6/day) (0-100, 100-200, 200-280 m; SF: 53-210, 210-560 µm)											36
	Naupliar Cohort (n = 3/day) (0-100, 100-200, 200-280 m)	**								**	**	12

Table 2. Copepod stage retention for small (53-210 µm) and medium (210-560 µm) zooplankton size fractions collected from January to March 2023 from Resurrection Bay, Alaska. Taxa not discussed in this paper are not included. Early and late nauplii are classified as NI-NIII and NIV-NVI stages, respectively. Copepods are classified as early (CI-CIII) and late (CIV-CVI adult) stages. Asterisks indicate rare occasions of stage presence within a size fraction.

		Size Fraction	
Taxa		Small (53-210 µm)	Medium (210-560 µm)
Nauplii	Calanoid	All stages	Late*
	Cyclopoid	All stages	--
Copepodites and Adults	**Small copepod taxa**		
	Oithona spp.	Early, Late	Early, Late
	Oncaeidae	Early, Late	Late*
	Pseudocalanus spp.	Early, Late*	Early, Late
	Large copepod taxa		
	Acartia longiremis	--	Early, Late
	Metridia pacifica	--	Early, Late
	Paraeuchaeta spp.	--	Early, Late
	Calanus marshallae	--	Early
	Metridia okhotensis	--	Early
	Neocalanus spp.	--	Early

Table 3. Summary statistics of naupliar length distributions from January to March 2023 collections at RES2.5. P-values for Kolmogrov Smirnov two-sided testing for significant differences in naupliar length distributions between sample dates and between neighboring depth strata within a sample date. P-values were calculated separately for calanoid and cyclopoid nauplii. Significant pairwise differences in distributions are bolded.

Pairwise comparison	Calanoida p-value	Cyclopoida p-value
By Date		
Jan 05: Feb22	0.294	**0.005**
Feb 22: Mar 24	**<0.001**	**<0.001**
Mar 24: Apr 22	0.602	**0.034**
By Depth		
January 5th		
0-100m: 100-200m	0.195	**0.010**
100-200m: 200-280m	0.296	0.150
February 22nd		
0-100m: 100-200m	0.623	0.433
100-200m: 200-280m	0.161	0.884
March 24th		
0-100m: 100-200m	**<0.001**	0.051
100-200m: 200-280m	0.354	**<0.001**

11 FIGURES

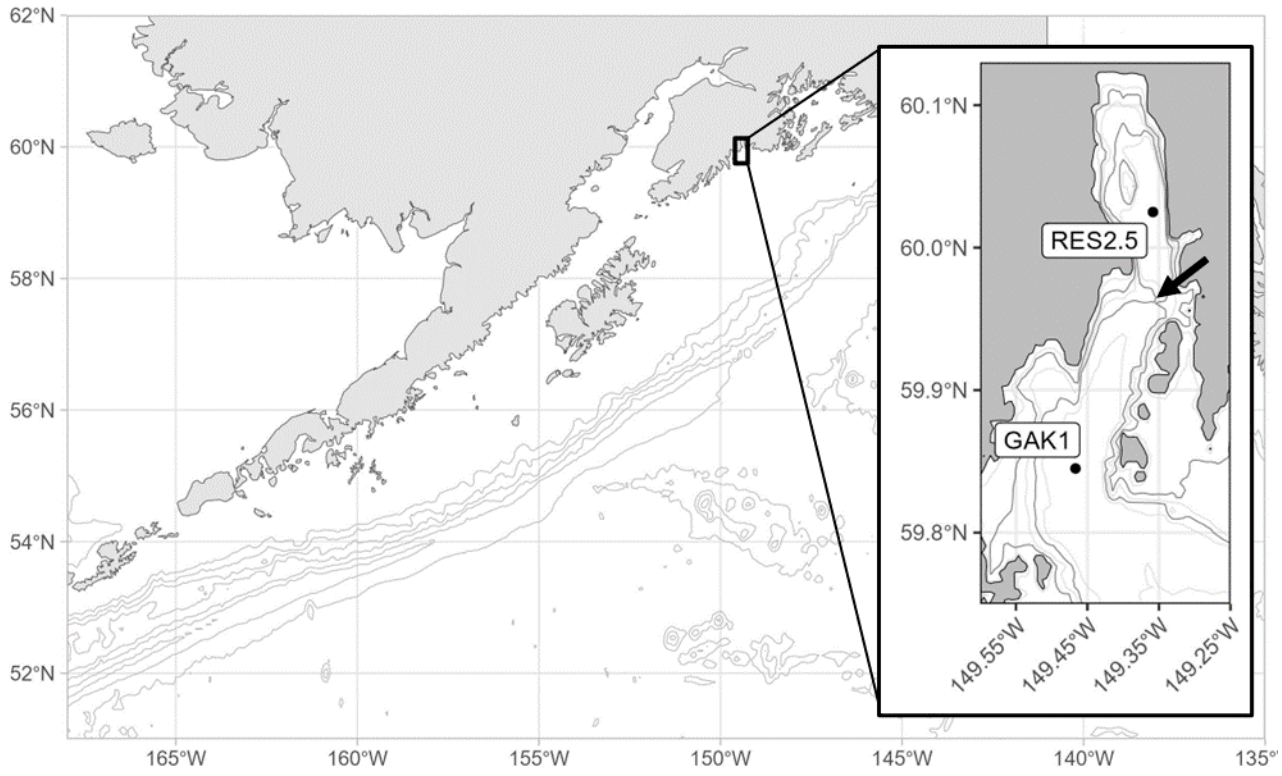

Figure 1. Map of the Gulf of Alaska and Resurrection Bay. 1000 m isobaths are marked. **Inset** locates Resurrection Bay, Alaska and sampling stations. Bathymetry on inset shows 50-meter isobaths with dark grey lines at 100 and 200 m depth. Arrow indicates sill at 185 m depth. Stations RES2.5 (60° 1.5'N, 149° 21.5'W) and GAK1 (59° 50.7'N, 149° 28.0'W) are marked.

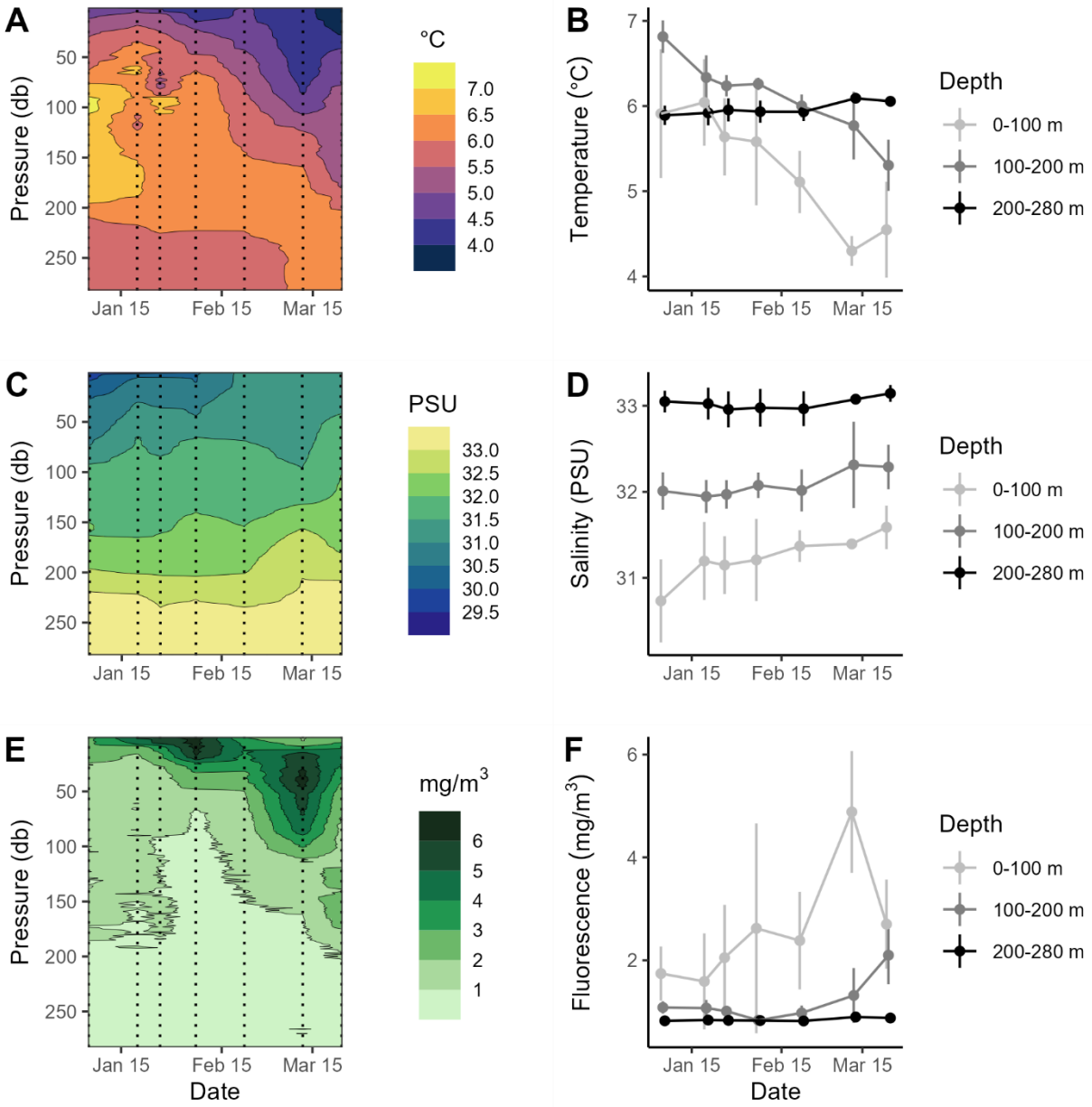

Figure 2. Environmental conditions at station RES2.5 in Resurrection Bay, AK during the 2023 study period. Depth (db) profiles of **(A)** temperature (°C), **(C)** salinity (PSU), and **(E)** fluorescence (mg/m^3) from January 5th to March 24th, 2023. Dotted lines mark individual CTD casts with data between the timepoints interpolated linearly. Mean **(B)** temperature, **(D)** salinity, and **(F)** fluorescence per depth strata (0-100, 100-200, and 200-280 m) over time. Error bars (B, D, and F) indicate ± standard deviation.

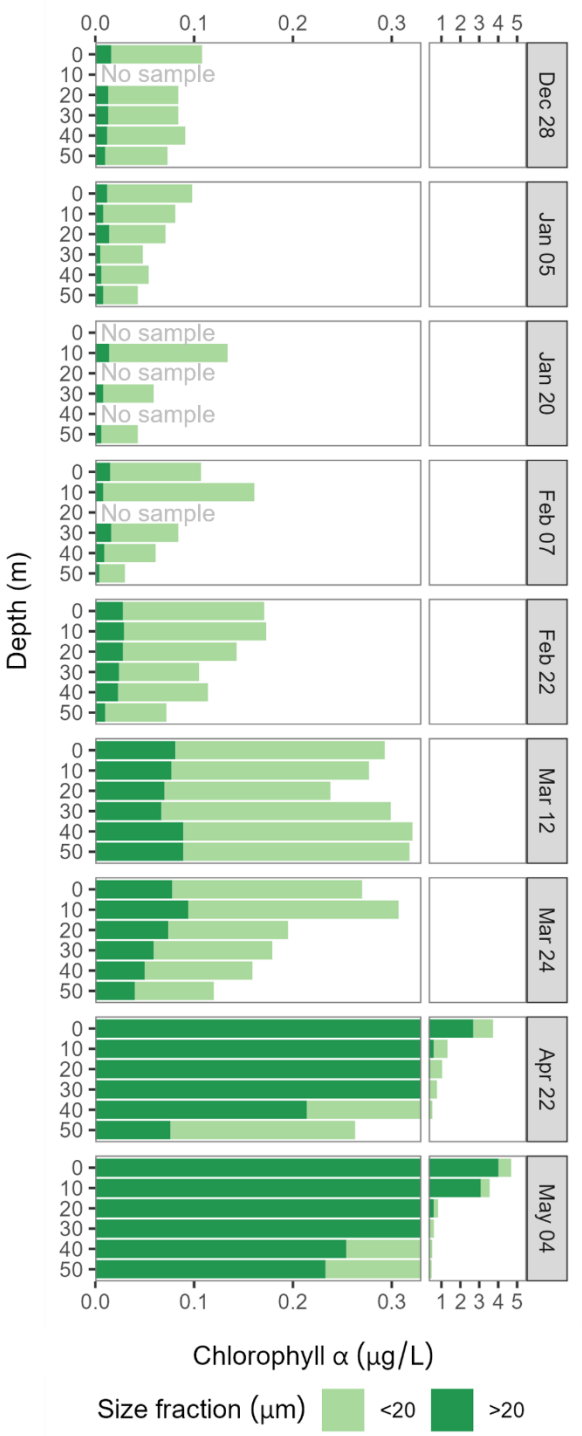

Figure 3. Chlorophyll α profiles in the upper 50 m at station RES2.5 in Resurrection Bay, AK. Bar graphs show size-fractionated chlorophyll α (µg/L) measurements from 6 discrete depths collected from December 28th, 2022, to May 4th, 2023. The x-axis contains a break at 0.33 µg/L (left panels) and a change in scale given the high chlorophyll α concentrations after the start of the bloom. April and May data were provided by Kerri Fredrickson and Suzanne Strom.

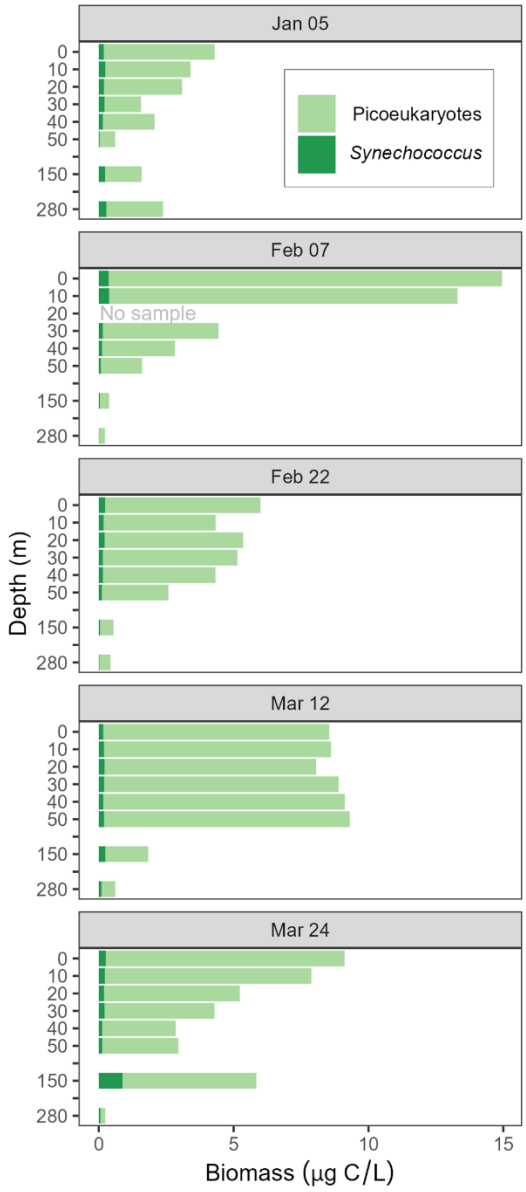

Figure 4. Profiles of photosynthetic picoeukaryote and *Synechococcus* biomass (µg C L^{-1}). Bar graphs show the vertical (8 depths) and temporal (5 dates) changes in biomass at station RES2.5 in Resurrection Bay, AK between January 5th and March 24th, 2023. Cell counts measured with flow cytometry were converted to carbon biomass (*Synechococcus:* 200 fg C per cell and picoeukaryote: 1,490 fg C per cell).

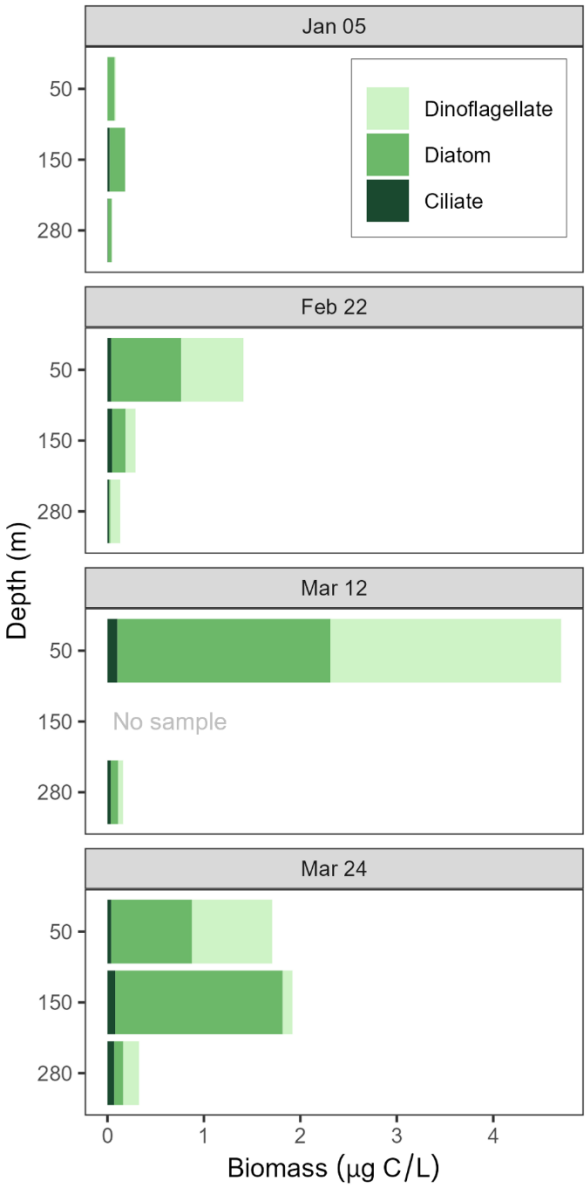

Figure 5. Biomass of ciliates, diatoms, and dinoflagellates at station RES2.5 in Resurrection Bay, AK between January and March 2023. Bar graphs show ciliate, diatom, and dinoflagellate biomass (µg C L^{-1}) enumerated from Acid-Lugol's-preserved samples from three depths and four dates. No sample was processed for the 150 m depth stratum on March 12th. Cell counts were converted into carbon biomass using established carbon to biovolume relationships.

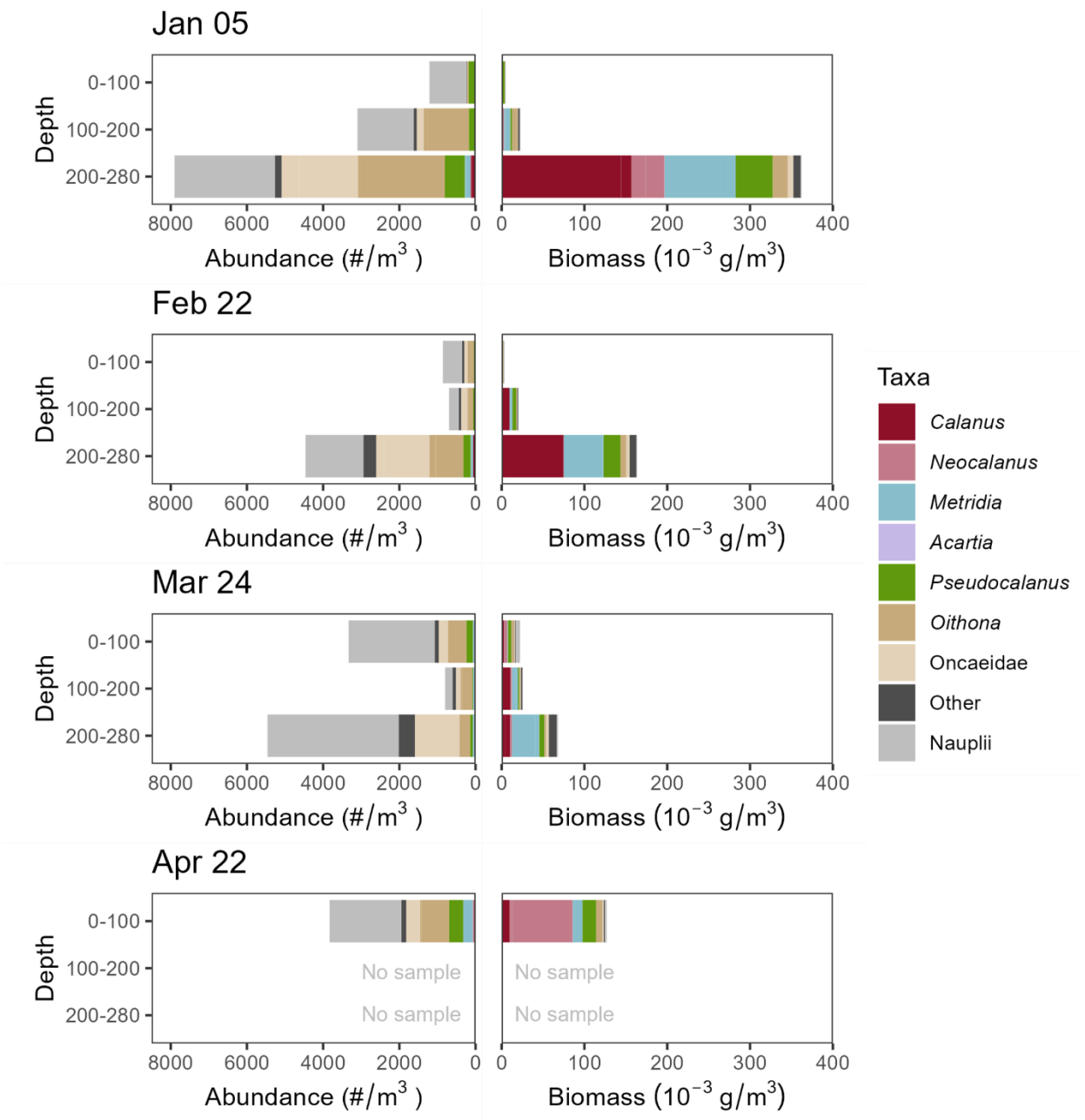

Figure 6. Vertical and temporal abundances and biomass of copepod taxa at station RES2.5 in Resurrection Bay, AK between early January and April were assessed using microscopy. Abundance (# per m^3) and biomass (10^{-3} g wet weight per m^3) of the total copepod community per depth strata (0-100, 100-200, 200-280 m) from January 5th to April 22nd, 2023. On April 22nd, zooplankton collection was limited to the 0-100 m stratum. Copepodite and adult copepod stages are colored by taxon. Total nauplii are plotted in gray. *Microcalanus*, *Microsetella*, *Candacia*, *Paraeuchaeta* and other taxa comprise the "other" category. Samples processed by Alex Poje and the Hopcroft lab.

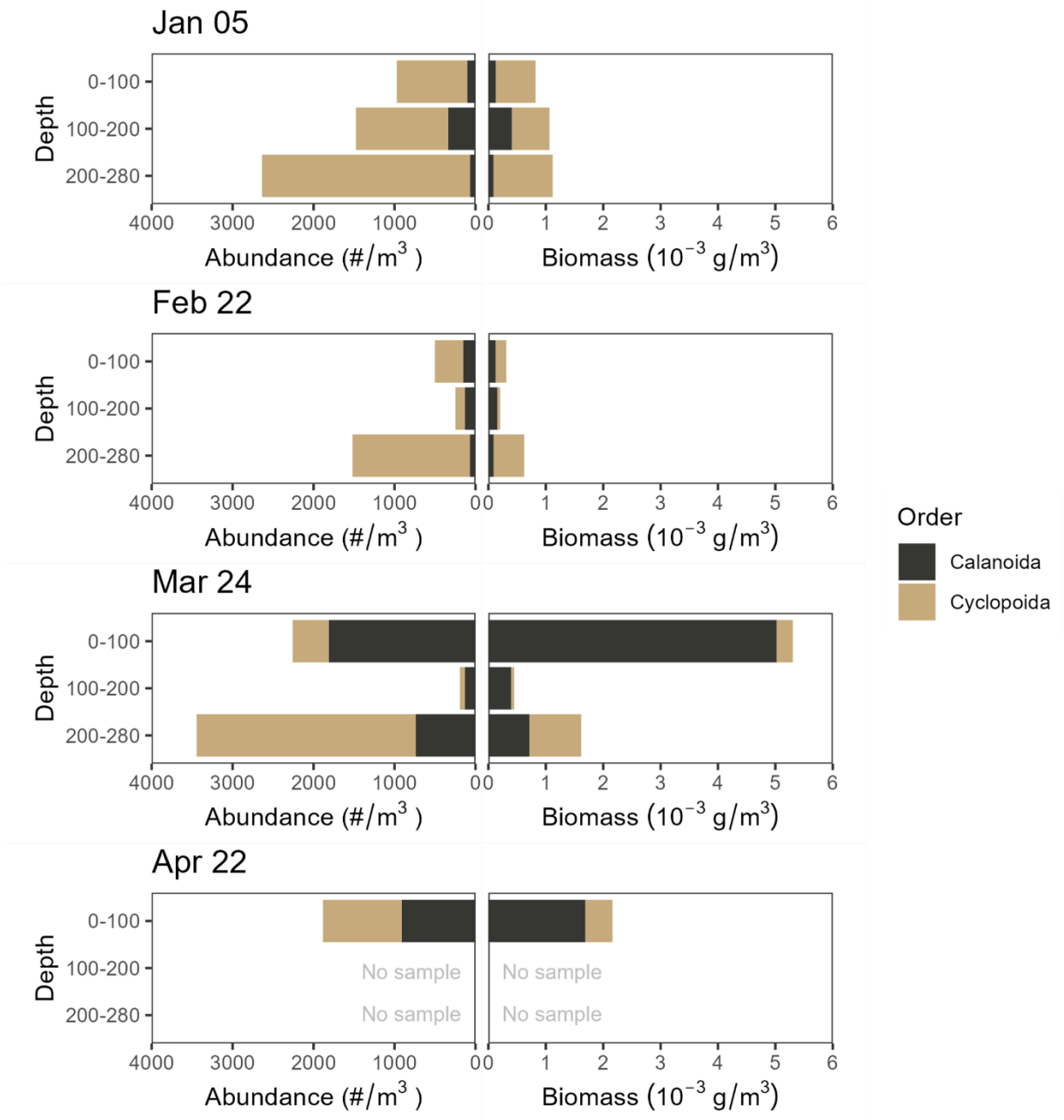

Figure 7. Calanoid and cyclopoid naupliar abundances and biomass at station RES2.5 in Resurrection Bay, AK. Abundance (# per m^3) and biomass (10^{-3} g wet weight per m^3) of nauplii per depth stratum (0-100, 100-200, 200-280 m) from January 5th to April 22nd, 2023. Only a 0-100 m sample was collected on April 22nd. Nauplii were identified to Order.

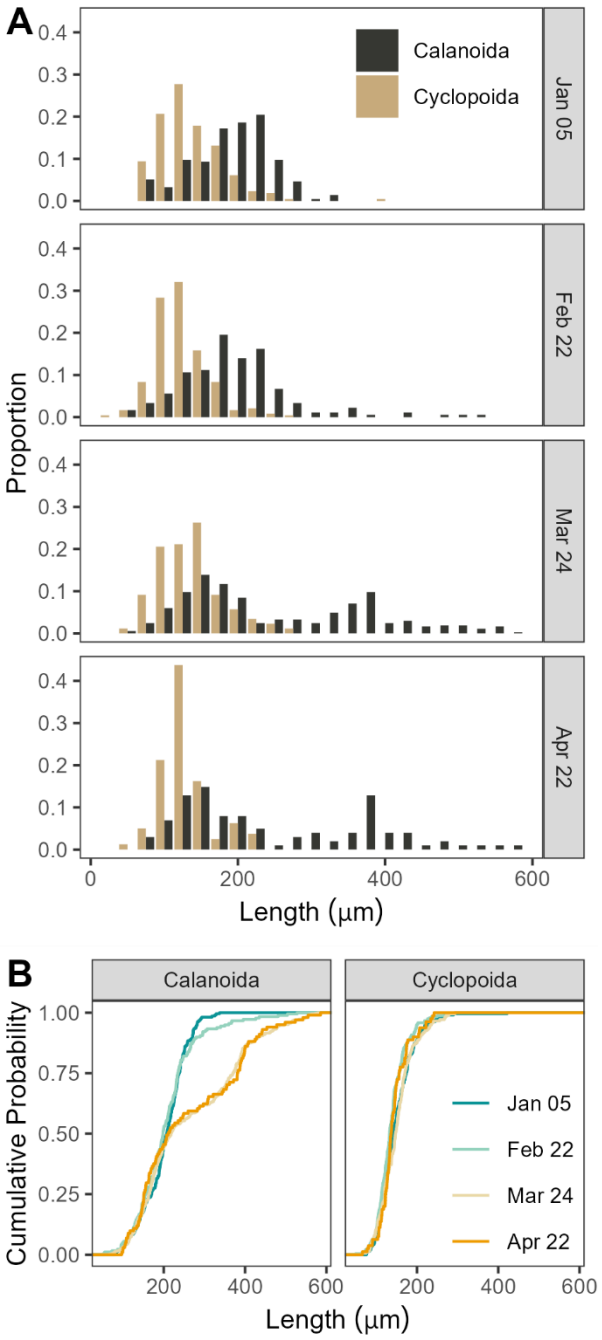

Figure 8. Naupliar size distributions at different collection times from early January to late April 2023, at station RES2.5 in Resurrection Bay, AK. **(A)** Length distributions of copepod nauplii measured from formalin-preserved samples represented as the proportion of nauplii collected per date within a length bin. Proportions were calculated separately for calanoid and cyclopoid nauplii. Samples were integrated over depth with the exception of April 22nd, which was only collected between 0-100 m. **(B)** Empirical cumulative distribution curves for calanoid and cyclopoid naupliar lengths for four sampling dates. Statistical tests are presented in Table 3.

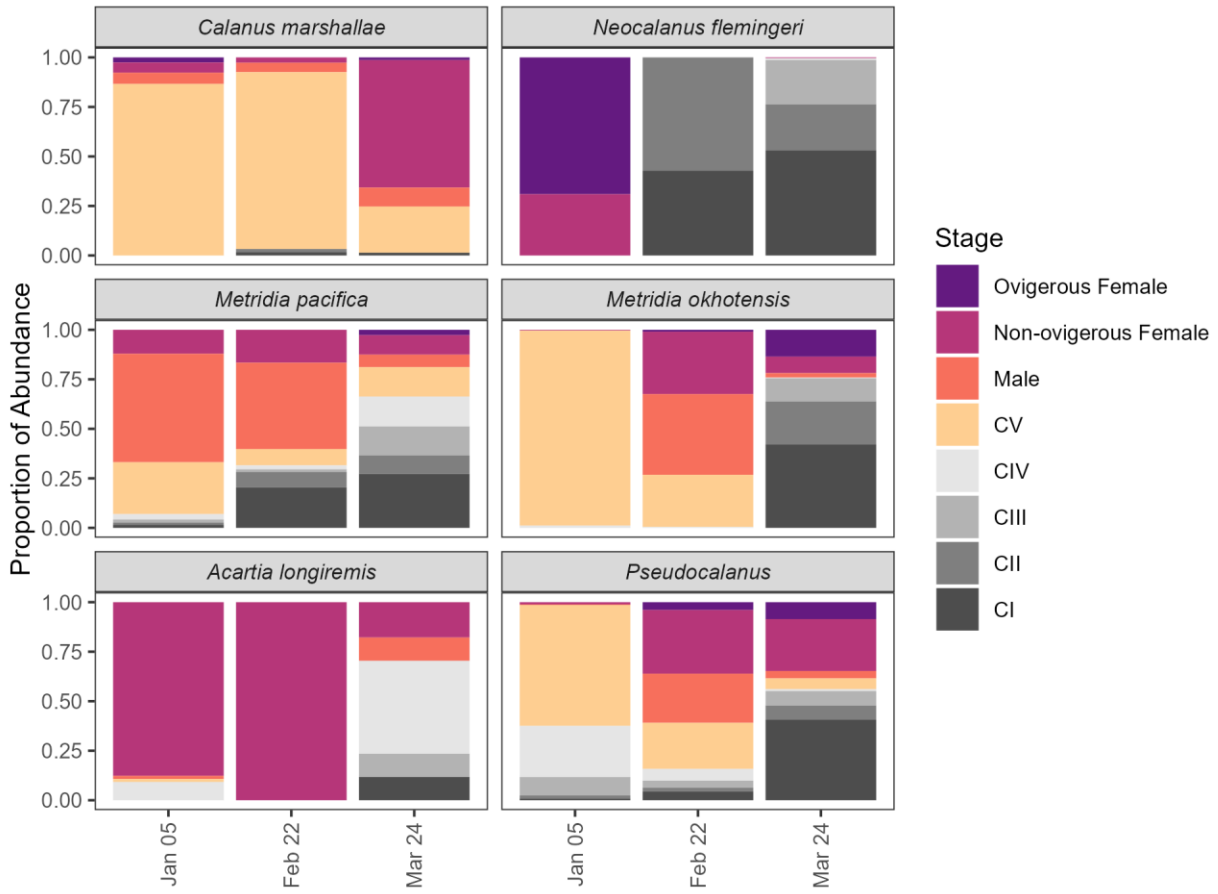

Figure 9. Stage composition of copepodites and adults of the dominant calanoid taxa from early January to late March 2023 at station RES2.5 in Resurrection Bay, AK. Stage distributions represent all three depth strata combined for each sample date. *Pseudocalanus* is combined for all species as CI-CV stages were not identified to species. Ovigerous and non-ovigerous females were distinguished in all cases except for *Acartia longiremis*.

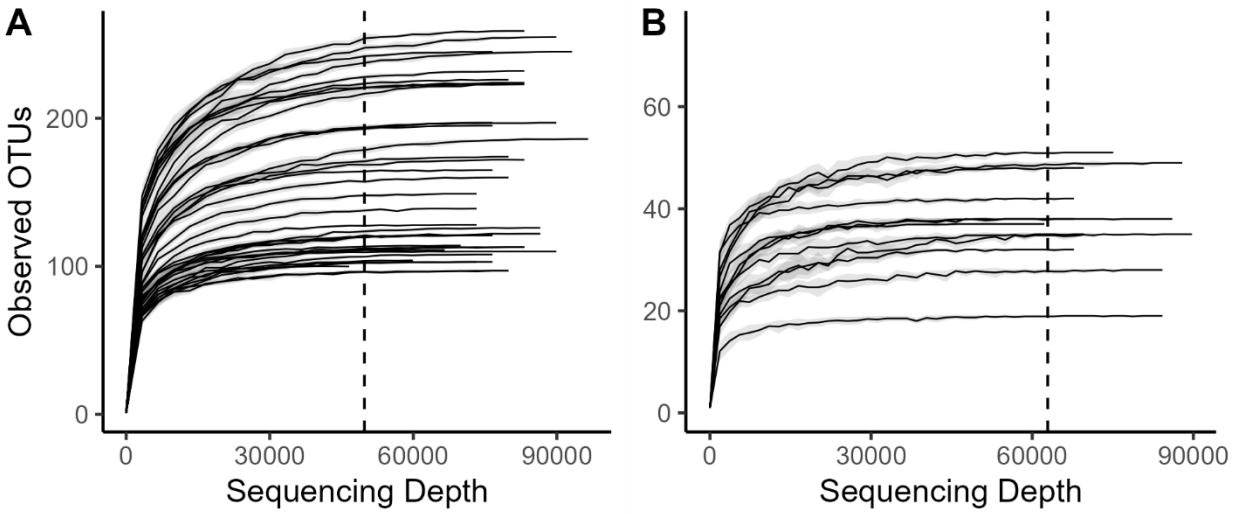

Figure 10. mCOI OTU rarefaction curves by sequencing depth (bp) for **(A)** bulk community metabarcoding samples and **(B)** naupliar cohort metabarcoding samples. Shaded regions represent standard deviations after 10 iterations. The vertical dashed line is positioned at the rarefaction depth. Samples collected between December 28th, 2022, and May 4th, 2023, at station RES2.5 in Resurrection Bay, AK.

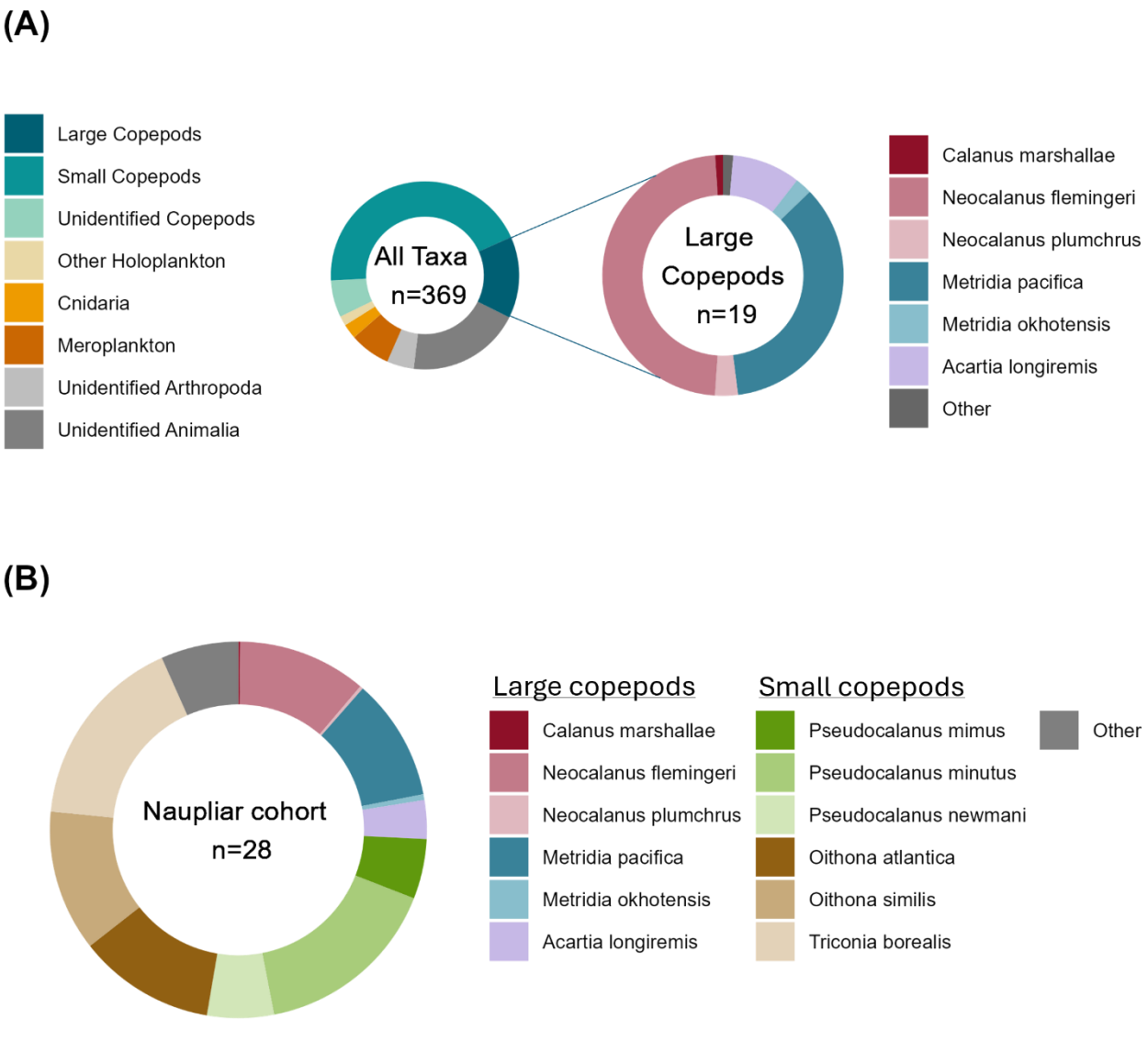

Figure 11. Overall taxonomic composition of DNA metabarcoding samples collected in winter 2023 from station RES2.5 in Resurrection Bay, AK. **(A)** Pie chart of small size fraction (53-210 µm) bulk community samples. All metazoan taxa present are grouped by broad functional groups (left) with the species composition of large copepods (right). **(B)** Pie chart of taxa present in naupliar cohort samples. Other includes minor contributing species and sequences not identified to the species level. n indicates the number of total unique taxa present.

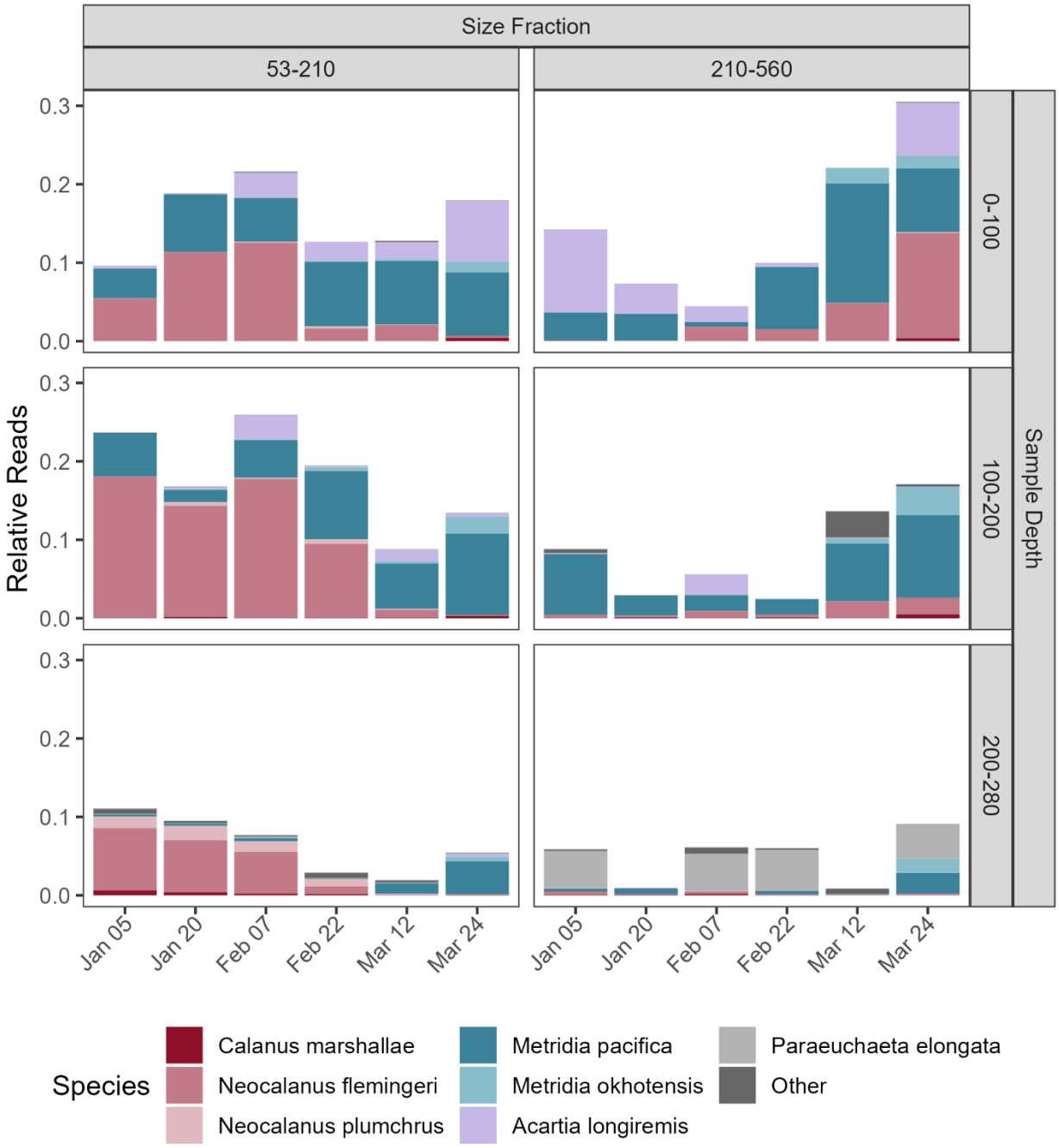

Figure 12. Relative read composition for large copepod species in size-fractionated bulk community metabarcoding samples. Relative reads represent the proportion of total sample reads from six collection dates between January 5th to March 24th, 2023, at station RES2.5 in Resurrection Bay, AK. Samples are split by depth strata (0-100 m, 100-200 m, and 200-280 m) in rows and size fraction (53-210 µm and 210-560 µm) in columns.

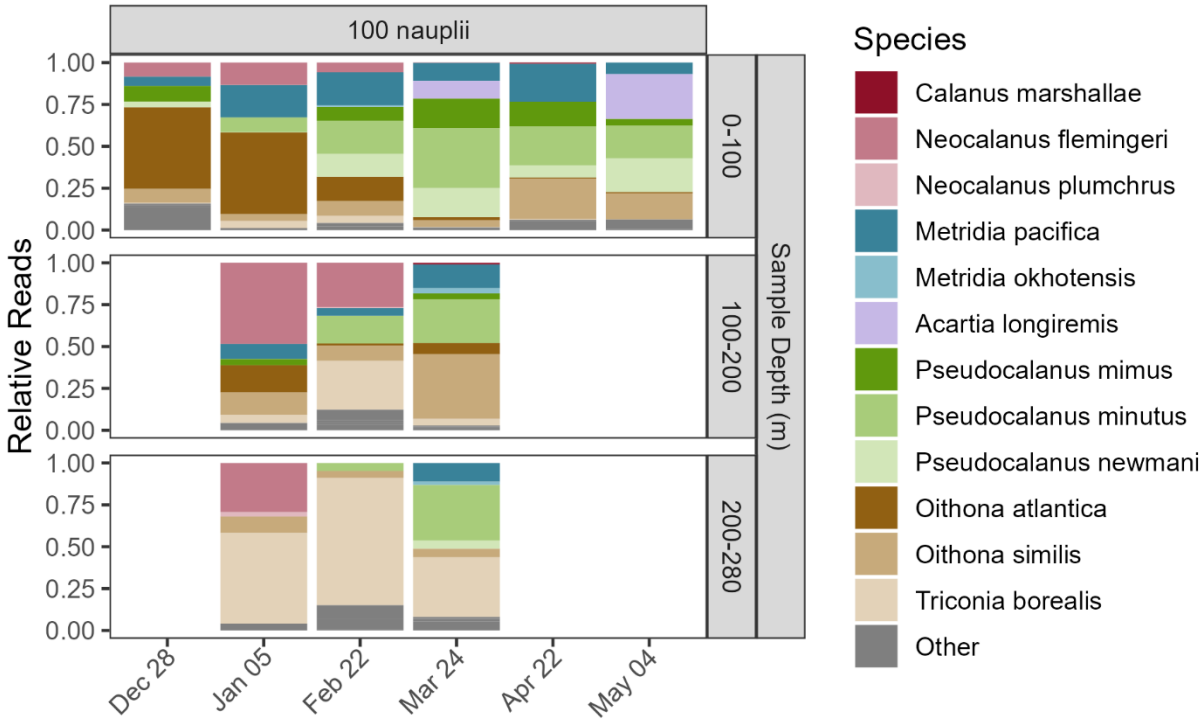

Figure 13. Relative read composition for naupliar cohort metabarcoding samples collected from station RES2.5 in Resurrection Bay, AK at six timepoints between December 2022 and May 2023. Relative reads are expressed as a fraction of total copepod reads. Samples are split by depth strata (0-100 m, 100-200 m, and 200-280 m).

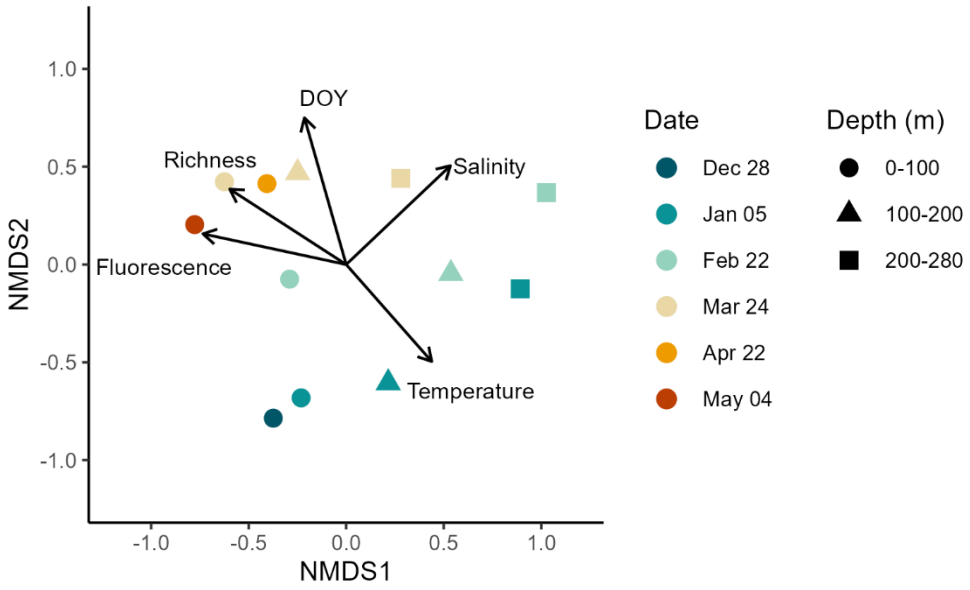

Figure 14. nMDS ordination of relative read composition from naupliar cohort samples collected from late December 2022 to early May 2023 at station RES2.5 in Resurrection Bay, AK. Sample dates are color-coded and depth strata are denoted by shapes. Vectors indicate the direction of steepest increase for continuous environmental parameters in ordination space. DOY = day of year.

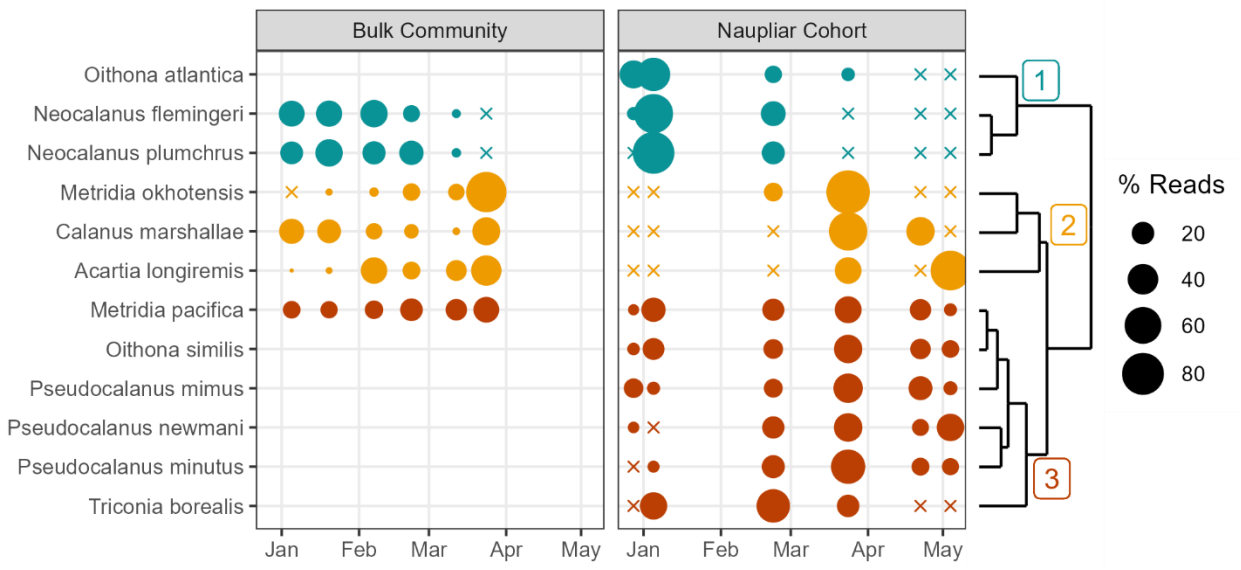

Figure 15. Ward's hierarchical cluster analysis of temporal changes in species prevalence based on metabarcoding samples collected between December 2022 and May 2023 at station RES2.5 in Resurrection Bay, AK. Data were normalized using a Wisconsin double transformation and the point size represents the percentage of a species' reads that are present on a given date. Xs indicate fewer than 1% of a species' sequences were present on a given date. Note that December, April, and May timepoints are limited to the 0-100 m depths strata. Species were clustered based on seasonal phenologies and the corresponding dendrogram is displayed on the right. The three clusters are labeled and points are colored according to their corresponding cluster.

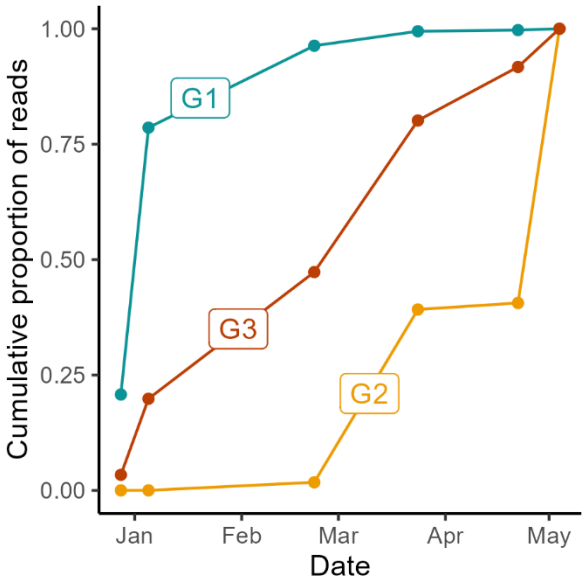

Figure 16. Cumulative proportion of naupliar cohort sample reads over time by species grouping. Groupings (G1, G2, & G3) determined by hierarchical cluster analysis (Figure 15). Samples collected between December 28th, 2022, and May 4th, 2023, at station RES2.5 in Resurrection Bay, AK. Note that January – March samples are comprised of all three depth strata whereas December, April, and May samples are limited to the 0-100 m depth strata.

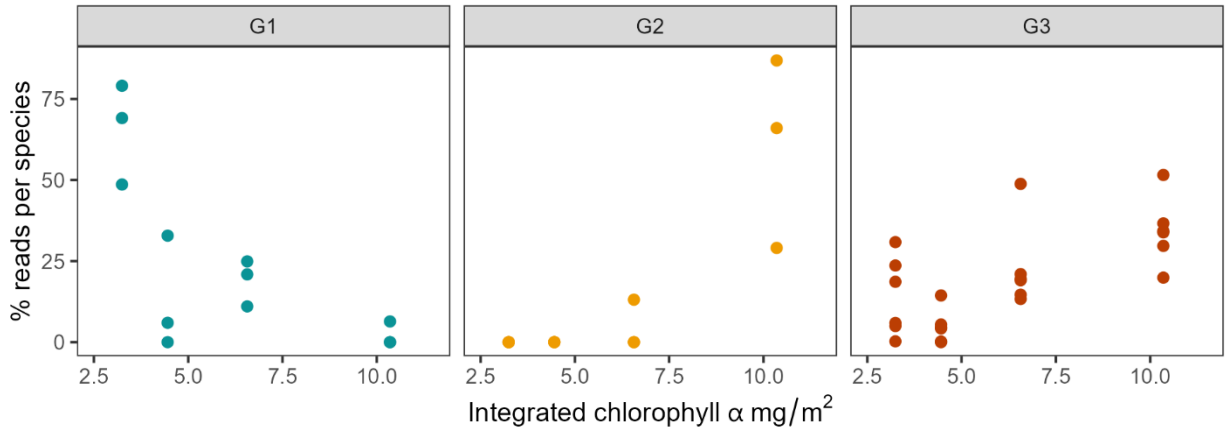

Figure 17. Relationship between depth-integrated chlorophyll α (mg/m^2) and relative species presence per species group between December 2022 and March 2023 station RES2.5 in Resurrection Bay, AK. Chlorophyll α was integrated from 0-50 m using the trapezoidal integration method. Relative species presence is an individual species' Wisconsin double standardized reads of naupliar cohort samples. Species groupings (G1, G2, & G3) were determined by hierarchical cluster analysis (Figure 15).

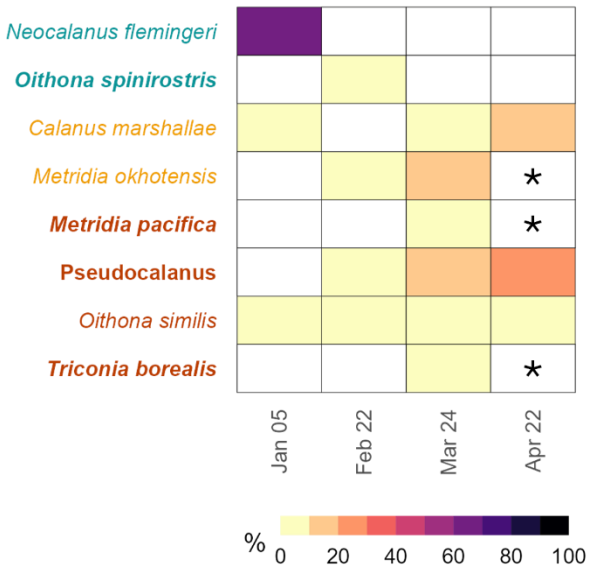

Figure 18. Percentage of ovigerous or egg-bearing females in a species' population between January 5th and April 22nd, 2023, at station RES2.5 in Resurrection Bay, AK. The three depth strata were combined for each sample date except April 22nd, which was limited to a 0-100 m sample. Asterisks indicate deep-water species with no females observed in the April 0-100 m sample. Taxa are ordered and color coded based on their naupliar phenology cluster (Figure 15). Taxa with a mismatch between the presence of nauplii and ovigerous females are bolded. *Pseudocalanus* is combined for all species as CI-CV stages were not distinguished to species-level. Ovigerous and non-ovigerous females were distinguished in all cases except for *Acartia longiremis*, which is not included.

12 APPENDICES

Appendix 1. Verification OTU identification for species discussed in naupliar cohort samples collected from RES2.5 between December 2022 and May 2023. For some species, multiple OTUs (clustered at 97% similarity) were identified. Percentage of species' reads indicates the percentage of total naupliar cohort sequences for the species that are attributed to a particular OTU. OTUs that make up less than 5% of a species' sequences are not shown below. QIIME confidence is output by the QIIME2 Naïve Bayes Classifier with 1 indicating highest confidence. Percent identity to NCBI and BOLD reference databases are shown for each OTU sequence.

OTU	Species Identification	Percentage of species' reads	QIIME confidence	NCBI percent identity	BOLD percent identity
1	*Neocalanus flemingeri*	76.2	1	100	100
2	*Neocalanus flemingeri*	21.7	1	99.60	100
3	*Neocalanus plumchrus*	72.6	1	100	100
4	*Neocalanus plumchrus*	10.0	1	99.70	98.69
5	*Neocalanus plumchrus*	6.9	1	100	100
6	*Calanus marshallae*	95.5	0.981	99.02	100
7	*Metridia pacifica*	99.9	1	100	97.99
8	*Metridia okhotensis*	99.7	1	100	100
9	*Acartia longiremis*	100.0	1	100	100
10	*Pseudocalanus mimus*	99.0	1	100	100
11	*Pseudocalanus minutus*	99.7	1	100	100
12	*Pseudocalanus newmani*	97.5	1	100	100
13	*Oithona atlantica*	99.8	1	NA	100
14	*Oithona similis*	53.0	1	100	NA
15	*Oithona similis*	47.0	1	96.09	NA
16	*Triconia borealis*	100	1	NA	99.02

Appendix 2. Table of relative reads (%) for large copepod species from bulk community metabarcoding samples (small 53-210 µm and medium 210-560 µm size fractions) collected at RES2.5 between January 5th and March 24th, 2023 from three depth strata (0-100 m, 100-200 m, and 200-280 m). See figure 12 for barplot.

	Small Size Fraction (53-210 µm)						Medium Size Fraction (210-560 µm)					
Species	Jan 05	Jan 20	Feb 07	Feb 22	Mar 12	Mar 24	Jan 05	Jan 20	Feb 07	Feb 22	Mar 12	Mar 24
0-100 m												
Calanus marshallae	0.0	0.0	0.0	0.0	0.0	0.7	0.0	0.0	0.0	0.0	0.0	0.6
Neocalanus flemingeri	8.7	20.8	23.4	3.0	3.3	0.3	0.1	0.0	1.8	2.4	7.7	20.6
Neocalanus plumchrus	0.0	0.0	0.2	0.5	0.1	0.0	0.0	0.0	0.0	0.0	0.0	0.1
Metridia pacifica	6.0	13.3	10.8	15.5	13.5	13.3	4.5	4.8	0.6	12.0	23.9	12.4
Metridia okhotensis	0.0	0.0	0.0	0.2	0.3	2.3	0.0	0.0	0.0	0.0	3.1	2.5
Acartia longiremis	0.6	0.3	6.1	4.3	3.6	13.2	13.3	5.6	2.0	0.7	0.0	10.2
Paraeuchaeta elongata	0.0	0.0	0.0	0.0	0.0	0.0	0.0	0.0	0.0	0.0	0.0	0.0
100-200 m												
Calanus marshallae	0.0	0.2	0.1	0.1	0.1	0.5	0.0	0.1	0.1	0.1	0.0	0.8
Neocalanus flemingeri	31.1	24.7	30.2	14.8	1.7	0.2	0.6	0.4	1.5	0.6	3.4	3.3
Neocalanus plumchrus	0.0	0.8	0.3	0.9	0.2	0.0	0.0	0.0	0.0	0.0	0.0	0.0
Metridia pacifica	9.7	2.6	8.2	13.6	9.4	16.7	10.4	4.0	3.5	3.2	11.6	15.9
Metridia okhotensis	0.0	0.1	0.1	0.7	0.4	3.3	0.0	0.0	0.0	0.0	1.1	5.5
Acartia longiremis	0.0	0.5	5.5	0.3	2.3	0.7	0.2	0.0	4.2	0.0	0.2	0.0
Paraeuchaeta elongata	0.0	0.0	0.1	0.0	0.1	0.2	0.0	0.0	0.1	0.0	0.0	0.0
200-280 m												
Calanus marshallae	1.1	0.7	0.3	0.2	0.0	0.1	0.1	0.1	0.4	0.1	0.0	0.0
Neocalanus flemingeri	13.5	12.7	8.5	1.5	0.2	0.1	0.7	0.1	0.6	0.1	0.0	0.3
Neocalanus plumchrus	2.5	3.5	2.1	1.5	0.1	0.0	0.0	0.0	0.3	0.0	0.0	0.0
Metridia pacifica	0.5	0.5	0.6	0.1	2.0	6.7	0.6	1.2	0.2	0.8	0.1	4.5
Metridia okhotensis	0.0	0.1	0.2	0.0	0.2	1.0	0.1	0.0	0.1	0.1	0.0	3.1
Acartia longiremis	0.0	0.0	0.0	0.0	0.0	0.6	0.0	0.0	0.0	0.0	0.0	0.0
Paraeuchaeta elongata	0.0	0.0	0.1	0.1	0.0	0.0	8.0	0.0	8.3	0.0	0.1	7.6

Appendix 3. Table of relative reads (%) for naupliar cohort metabarcoding samples collected at RES2.5 between December 28th, 2022 and May 4th, 2023 from three depth strata (0-100 m, 100-200 m, and 200-280 m). No samples were collected below 100 m on December 28th, April 22nd, or May 4th. See figure 13 for barplot.

Species	Dec 28	Jan 05	Feb 22	Mar 24	Apr 22	May 04
0-100 m						
Calanus marshallae	0.0	0.0	0.0	0.1	0.6	0.0
Neocalanus flemingeri	7.3	13.1	5.2	0.0	0.0	0.0
Neocalanus plumchrus	0.0	0.0	0.0	0.0	0.0	0.0
Metridia pacifica	4.9	19.0	17.7	10.6	20.3	6.6
Metridia okhotensis	0.0	0.0	0.7	0.0	0.0	0.0
Acartia longiremis	0.0	0.0	0.0	10.7	0.0	26.0
Pseudocalanus mimus	8.2	0.0	7.5	17.5	13.0	3.8
Pseudocalanus minutus	0.0	8.8	17.6	35.6	20.8	18.9
Pseudocalanus newmani	2.9	0.2	12.3	17.2	6.6	19.6
Oithona atlantica	42.5	47.7	13.0	1.8	0.6	0.8
Oithona similis	7.3	4.0	7.9	4.0	21.5	15.1
Triconia borealis	0.4	4.2	3.8	0.2	0.4	0.0
100-200 m						
Calanus marshallae	--	0.0	0.0	0.9	--	--
Neocalanus flemingeri	--	45.0	25.1	0.0	--	--
Neocalanus plumchrus	--	0.0	0.6	0.0	--	--
Metridia pacifica	--	8.4	4.3	13.4	--	--
Metridia okhotensis	--	0.0	0.0	3.0	--	--
Acartia longiremis	--	0.0	0.0	0.0	--	--
Pseudocalanus mimus	--	3.4	0.0	3.3	--	--
Pseudocalanus minutus	--	0.0	15.7	24.8	--	--
Pseudocalanus newmani	--	0.0	0.0	0.0	--	--
Oithona atlantica	--	15.2	1.2	6.4	--	--
Oithona similis	--	12.3	8.5	36.6	--	--
Triconia borealis	--	4.5	27.8	3.8	--	--
200-280 m						
Calanus marshallae	--	0.0	0.0	0.0	--	--
Neocalanus flemingeri	--	26.1	0.0	0.0	--	--
Neocalanus plumchrus	--	2.4	0.0	0.0	--	--
Metridia pacifica	--	0.0	0.0	10.3	--	--
Metridia okhotensis	--	0.0	0.0	1.7	--	--
Acartia longiremis	--	0.0	0.0	0.0	--	--
Pseudocalanus mimus	--	0.0	0.0	0.0	--	--
Pseudocalanus minutus	--	0.0	3.7	30.7	--	--
Pseudocalanus newmani	--	0.0	0.0	4.4	--	--
Oithona atlantica	--	0.0	0.0	0.0	--	--
Oithona similis	--	8.6	3.2	4.6	--	--
Triconia borealis	--	48.3	58.7	32.8	--	--

13 REFERENCES

Alix, M., Kjesbu, O.S., Anderson, K.C., 2020. From gametogenesis to spawning: How climate-driven warming affects teleost reproductive biology. Journal of Fish Biology 97, 607–632. https://doi.org/10.1111/jfb.14439

Arima, D., Yamaguchi, A., Nobetsu, T., Imai, I., 2016. Seasonal abundance, population structure, sex ratio and gonad maturation of *Metridia okhotensis* Brodsky, 1950 in the Okhotsk Sea: analysis of samples collected by pumping up from deep water. Crustaceana 89, 151–161. https://doi.org/10.1163/15685403-00003516

Arimitsu, M.L., Piatt, J.F., Hatch, S., Suryan, R.M., Batten, S., Bishop, M.A., Campbell, R.W., Coletti, H., Cushing, D., Gorman, K., Hopcroft, R.R., Kuletz, K.J., Marsteller, C., McKinstry, C., McGowan, D., Moran, J., Pegau, S., Schaefer, A., Schoen, S., Straley, J., Biela, V.R. von, 2021. Heatwave-induced synchrony within forage fish portfolio disrupts energy flow to top pelagic predators. Global Change Biology 27, 1859–1878. https://doi.org/10.1111/gcb.15556

Atkinson, A., 1998. Life cycle strategies of epipelagic copepods in the Southern Ocean. Journal of Marine Systems 15, 289–311. https://doi.org/10.1016/S0924-7963(97)00081-X

Baier, C.T., Napp, J.M., 2003. Climate-induced variability in *Calanus marshallae* populations. Journal of Plankton Research 25, 771–782. https://doi.org/10.1093/plankt/25.7.771

Balazy, K., Boehnke, R., Trudnowska, E., Søreide, J.E., Błachowiak-Samołyk, K., 2021. Phenology of *Oithona similis* demonstrates that ecological flexibility may be a winning trait in the warming Arctic. Scientific Reports 11, 18599. https://doi.org/10.1038/s41598-021-98068-8

Ballantine, K., 2024. Investigating physical drivers of phytoplankton bloom initiation in the Northern Gulf of Alaska (Honor's). Oregon State University.

Batchelder, H.P., 1985. Seasonal abundance, vertical distribution, and life history of *Metridia pacifica* (Copepoda: Calanoida) in the oceanic subarctic Pacific. Deep Sea Research Part A. Oceanographic Research Papers 32, 949–964. https://doi.org/10.1016/0198-0149(85)90038-X

Baumgartner, M.F., Tarrant, A.M., 2017. The physiology and ecology of diapause in marine copepods. Annual Review of Marine Science 9, 387–411. https://doi.org/10.1146/annurev-marine-010816-060505

Behrenfeld, M.J., 2010. Abandoning Sverdrup's critical depth hypothesis on phytoplankton blooms. Ecology 91, 977–989.

Biggs, C.R., Yeager, L.A., Bolser, D.G., Bonsell, C., Dichiera, A.M., Hou, Z., Keyser, S.R., Khursigara, A.J., Lu, K., Muth, A.F., Negrete, B., Erisman, B.E., 2020. Does functional redundancy affect ecological stability and resilience? A review and meta-analysis. Ecosphere 11, 1–9. https://doi.org/10.1002/ecs2.3184

Bolyen, E., Rideout, J.R., Dillon, M.R., Bokulich, N.A., Abnet, C.C., Al-Ghalith, G.A., Alexander, H., Alm, E.J., Arumugam, M., Asnicar, F., Bai, Y., Bisanz, J.E., Bittinger, K., Brejnrod, A., Brislawn, C.J., Brown, C.T., Callahan, B.J., Caraballo-Rodríguez, A.M., Chase, J., Cope, E.K., Da Silva, R., Diener, C., Dorrestein, P.C., Douglas, G.M., Durall, D.M., Duvallet, C., Edwardson, C.F., Ernst, M., Estaki, M., Fouquier, J., Gauglitz, J.M., Gibbons, S.M., Gibson, D.L., Gonzalez, A., Gorlick, K., Guo, J., Hillmann, B., Holmes, S., Holste, H., Huttenhower, C., Huttley, G.A., Janssen, S., Jarmusch, A.K., Jiang, L., Kaehler, B.D., Kang, K.B., Keefe, C.R., Keim, P., Kelley, S.T., Knights, D., Koester, I., Kosciolek, T., Kreps, J., Langille, M.G.I., Lee, J., Ley, R., Liu, Y.-X., Loftfield, E., Lozupone, C., Maher, M., Marotz, C., Martin, B.D., McDonald, D., McIver, L.J., Melnik, A.V., Metcalf, J.L., Morgan, S.C., Morton, J.T., Naimey, A.T., Navas-Molina, J.A., Nothias, L.F., Orchanian, S.B., Pearson, T., Peoples, S.L., Petras, D., Preuss, M.L., Pruesse, E., Rasmussen,

L.B., Rivers, A., Robeson, M.S., Rosenthal, P., Segata, N., Shaffer, M., Shiffer, A., Sinha, R., Song, S.J., Spear, J.R., Swafford, A.D., Thompson, L.R., Torres, P.J., Trinh, P., Tripathi, A., Turnbaugh, P.J., Ul-Hasan, S., van der Hooft, J.J.J., Vargas, F., Vázquez-Baeza, Y., Vogtmann, E., von Hippel, M., Walters, W., Wan, Y., Wang, M., Warren, J., Weber, K.C., Williamson, C.H.D., Willis, A.D., Xu, Z.Z., Zaneveld, J.R., Zhang, Y., Zhu, Q., Knight, R., Caporaso, J.G., 2019. Reproducible, interactive, scalable and extensible microbiome data science using QIIME 2. Nature Biotechnology 37, 852–857. https://doi.org/10.1038/s41587-019-0209-9

Brickley, P.J., Thomas, A.C., 2004. Satellite-measured seasonal and inter-annual chlorophyll variability in the Northeast Pacific and coastal Gulf of Alaska. Deep Sea Research Part II: Topical Studies in Oceanography 51, 229–245. https://doi.org/10.1016/j.dsr2.2003.06.003

Bucklin, A., 2000. Methods for population genetic analysis of zooplankton, in: Harris, R., Wiebe, P., Lenz, J., Skjoldal, H.R., Huntley, M. (Eds.), ICES Zooplankton Methodology Manual. Academic Press, London, pp. 533–570. https://doi.org/10.1016/B978-012327645-2/50012-8

Bucklin, A., Guarnieri, M., McGillicuddy, D.J., Sean Hill, R., 2001. Spring evolution of Pseudocalanus spp. abundance on Georges Bank based on molecular discrimination of P. moultoni and P. newmani. Deep Sea Research Part II: Topical Studies in Oceanography, Coupled biological and physical studies of plankton populations on Georges Bank and related North Atlantic regions 48, 589–608. https://doi.org/10.1016/S0967-0645(00)00128-4

Bucklin, A., Peijnenburg, K.T.C.A., Kosobokova, K.N., O'Brien, T.D., Blanco-Bercial, L., Cornils, A., Falkenhaug, T., Hopcroft, R.R., Hosia, A., Laakmann, S., Li, C., Martell, L., Questel, J.M., Wall-Palmer, D., Wang, M., Wiebe, P.H., Weydmann-Zwolicka, A., 2021. Toward a global reference database of COI barcodes for marine zooplankton. Marine Biology 168, 78. https://doi.org/10.1007/s00227-021-03887-y

Callahan, B.J., McMurdie, P.J., Rosen, M.J., Han, A.W., Johnson, A.J.A., Holmes, S.P., 2016. DADA2: High-resolution sample inference from Illumina amplicon data. Nature Methods 13, 581–583. https://doi.org/10.1038/nmeth.3869

Castellani, C., Irigoien, X., Harris, R.P., Holliday, N.P., 2007. Regional and temporal variation of *Oithona* spp. biomass, stage structure and productivity in the Irminger Sea, North Atlantic. Journal of Plankton Research 29, 1051–1070. https://doi.org/10.1093/plankt/fbm079

Childers, A.R., Whitledge, T.E., Stockwell, D.A., 2005. Seasonal and interannual variability in the distribution of nutrients and chlorophyll *a* across the Gulf of Alaska shelf: 1998–2000. Deep Sea Research Part II: Topical Studies in Oceanography 52, 193–216. https://doi.org/10.1016/j.dsr2.2004.09.018

Conover, R.J., 1988. Comparative life histories in the genera *Calanus* and *Neocalanus* in high latitudes of the northern hemisphere. Hydrobiologia 167, 127–142. https://doi.org/10.1007/BF00026299

Cooney, R.T., Coyle, K.O., Stockmar, E., Stark, C., 2001. Seasonality in surface-layer net zooplankton communities in Prince William Sound, Alaska. Fisheries Oceanography 10, 97–109. https://doi.org/10.1046/j.1054-6006.2001.00037.x

Coyle, K.O., Pinchuk, A.I., 2005. Seasonal cross-shelf distribution of major zooplankton taxa on the northern Gulf of Alaska shelf relative to water mass properties, species depth preferences and vertical migration behavior. Deep Sea Research Part II: Topical Studies in Oceanography 52, 217–245. https://doi.org/10.1016/j.dsr2.2004.09.025

Coyle, K.O., Pinchuk, A.I., 2003. Annual cycle of zooplankton abundance, biomass and production on the northern Gulf of Alaska shelf, October 1997 through October 2000. Fisheries Oceanography 12, 327–338. https://doi.org/10.1046/j.1365-2419.2003.00256.x

Doyle, M.J., Mier, K.L., 2016. Early life history pelagic exposure profiles of selected commercially important fish species in the Gulf of Alaska. Deep Sea Research Part II: Topical Studies in Oceanography 132, 162–193. https://doi.org/10.1016/j.dsr2.2015.06.019

Doyle, M.J., Strom, S.L., Coyle, K.O., Hermann, A.J., Ladd, C., Matarese, A.C., Shotwell, S.K., Hopcroft, R.R., 2019. Early life history phenology among Gulf of Alaska fish species: Strategies, synchronies, and sensitivities. Deep Sea Research Part II: Topical Studies in Oceanography 165, 41–73. https://doi.org/10.1016/j.dsr2.2019.06.005

Dvoretsky, V.G., Dvoretsky, A.G., 2009. Life cycle of *Oithona similis* (Copepoda: Cyclopoida) in Kola Bay (Barents Sea). Marine Biology 156, 1433–1446. https://doi.org/10.1007/s00227-009-1183-4

Ershova, E.A., Questel, J.M., Kosobokova, K., Hopcroft, R.R., 2017. Population structure and production of four sibling species of *Pseudocalanus* spp. in the Chukchi Sea. Journal of Plankton Research 39, 48–64. https://doi.org/10.1093/plankt/fbw078

Ershova, E.A., Wangensteen, O.S., Descoteaux, R., Barth-Jensen, C., Præbel, K., 2021. Metabarcoding as a quantitative tool for estimating biodiversity and relative biomass of marine zooplankton. ICES Journal of Marine Science 78, 3342–3355. https://doi.org/10.1093/icesjms/fsab171

Etherington, L.L., Hooge, P.N., Hooge, E.R., Hill, D.F., 2007. Oceanography of Glacier Bay, Alaska: Implications for biological patterns in a glacial fjord estuary. Estuaries and Coasts 30, 927–944. https://doi.org/10.1007/BF02841386

Figge, F., 2004. Bio-folio: applying portfolio theory to biodiversity. Biodiversity and Conservation 13, 827–849. https://doi.org/10.1023/B:BIOC.0000011729.93889.34

Fujioka, H.A., Machida, R.J., Tsuda, A., 2015. Early life history of *Neocalanus plumchrus* (Calanoida: Copepoda) in the western subarctic Pacific. Progress in Oceanography 137, 196–208. https://doi.org/10.1016/j.pocean.2015.06.004

Gardner, G.A., Szabo, I., 1982. British Columbia pelagic marine copepoda: an identification manual and annotated bibliography, Canadian special publication of fisheries and aquatic sciences. Dept. of Fisheries and Oceans, Ottawa.

Hattori, H., 1989. Bimodal vertical distribution and diel migration of the copepods *Metridia pacifica*, *M. okhotensis* and *Pleuromamma scutullata* in the western North Pacific Ocean. Marine Biology 103, 39–50. https://doi.org/10.1007/BF00391063

Heggie, D.T., Boisseau, D.W., Burrell, D.C., 1977. Hydrography, nutrient chemistry, and primary productivity of Resurrection Bay, Alaska 1972-75 (IMS Report No. R77-2). University of Alaska, Institute of Marine Science.

Heggie, D.T., Burrell, D.C., 1981. Deep water renewals and oxygen consumption in an Alaskan fjord. Estuarine, Coastal and Shelf Science 13, 83–99. https://doi.org/10.1016/S0302-3524(81)80107-7

Heinrich, A.K., 1962. The Life Histories of Plankton Animals and Seasonal Cycles of Plankton Communities in the Oceans. ICES Journal of Marine Science 27, 15–24. https://doi.org/10.1093/icesjms/27.1.15

Hillebrand, H., Dürselen, C.-D., Kirschtel, D., Pollingher, U., Zohary, T., 1999. Biovolume calculation for pelagic and benthic microalgae. Journal of Phycology 35, 403–424. https://doi.org/10.1046/j.1529-8817.1999.3520403.x

Hirche, H.-J., 1996. The reproductive biology of the marine copepod, *Calanus finmarchicus* — A review. Ophelia 44, 111–128. https://doi.org/10.1080/00785326.1995.10429842

Hopcroft, R., Clarke Hopcroft, C., 2019. Seward Line zooplankton biomass and abundance data from spring and summer cruises aboard the Tiglax, 2012 to 2017, Gulf Watch Alaska Environmental Drivers component. https://doi.org/10.24431/RW1K32J

Hopcroft, R.R., 2021. Zooplankton abundance and biomass observations obtained from the QuadNet, as analyzed by traditional microscopy, during NGA LTER seasonal cruises in the Northern Gulf of Alaska, 2018-2019. https://doi.org/10.24431/RW1K587
Hopcroft, R.R., Clarke, C., Byrd, A.G., Pinchuk, A.I., 2005. The paradox of *Metridia* spp. egg production rates: a new technique and measurements from the coastal Gulf of Alaska. Marine Ecology Progress Series 286, 193–201. https://doi.org/10.3354/meps286193
Hopcroft, R.R., Roff, J.C., Lombard, D., 1998. Production of tropical copepods in Kingston Harbour, Jamaica: the importance of small species. Marine Biology 130, 593–604. https://doi.org/10.1007/s002270050281
Hutchinson, G.E., 1961. The paradox of the plankton. The American Naturalist 95, 137–145.
Hwang, J.-S., Kumar, R., Dahms, H.-U., Tseng, L.-C., Chen, Q.-C., 2010. Interannual, seasonal, and diurnal variations in vertical and horizontal distribution patterns of 6 *Oithona* spp. (Copepoda: Cyclopoida) in the South China Sea. Zoological Studies 49, 220–229.
Jönsson, K.I., 1997. Capital and income breeding as alternative tactics of resource use in reproduction. Oikos 78, 57–66. https://doi.org/10.2307/3545800
Kassambara, A., 2023. ggpubr: "ggplot2" based publication ready plots. R package version 0.6.0, <https://CRAN.R-project.org/package=ggpubr>.
Kelly, R.P., Shelton, A.O., Gallego, R., 2019. Understanding PCR processes to draw meaningful conclusions from environmental DNA studies. Scientific Reports 9, 12133. https://doi.org/10.1038/s41598-019-48546-x
Kimmel, D.G., Duffy-Anderson, J.T., 2020. Zooplankton abundance trends and patterns in Shelikof Strait, western Gulf of Alaska, USA, 1990–2017. Journal of Plankton Research 42, 334–354. https://doi.org/10.1093/plankt/fbaa019
Kobari, T., Ikeda, T., 2001. Life cycle of *Neocalanus flemingeri* (Crustacea: Copepoda) in the Oyashio region, western subarctic Pacific, with notes on its regional variations. Marine Ecology Progress Series 209, 243–255. https://doi.org/10.3354/meps209243
Lamb, P.D., Hunter, E., Pinnegar, J.K., Creer, S., Davies, R.G., Taylor, M.I., 2019. How quantitative is metabarcoding: A meta-analytical approach. Molecular Ecology 28, 420–430. https://doi.org/10.1111/mec.14920
Landry, M.R., Fagerness, V.L., 1988. Behavioral and morphological influences on predatory interactions among marine copepods. Bulletin of Marine Science 43, 509–529.
Lenz, P.H., Roncalli, V., 2019. Diapause within the context of life-history strategies in calanid copepods (Calanoida: Crustacea). The Biological Bulletin 237, 170–179. https://doi.org/10.1086/705160
Leray, M., Yang, J.Y., Meyer, C.P., Mills, S.C., Agudelo, N., Ranwez, V., Boehm, J.T., Machida, R.J., 2013. A new versatile primer set targeting a short fragment of the mitochondrial COI region for metabarcoding metazoan diversity: application for characterizing coral reef fish gut contents. Frontiers in Zoology 10, 1–14. https://doi.org/10.1186/1742-9994-10-34
Lindegren, M., Checkley, D.M., Ohman, M.D., Koslow, J.A., Goericke, R., 2016. Resilience and stability of a pelagic marine ecosystem. Proceedings of the Royal Society B: Biological Sciences 283, 20151931. https://doi.org/10.1098/rspb.2015.1931
Lischka, S., Hagen, W., 2005. Life histories of the copepods *Pseudocalanus minutus*, *P. acuspes* (Calanoida) and *Oithona similis* (Cyclopoida) in the Arctic Kongsfjorden (Svalbard). Polar Biology 28, 910–921. https://doi.org/10.1007/s00300-005-0017-1
Liu, H., Hopcroft, R.R., 2006. Growth and development of *Neocalanus flemingeri/plumchrus* in the northern Gulf of Alaska: validation of the artificial-cohort method in cold waters. Journal of Plankton Research 28, 87–101. https://doi.org/10.1093/plankt/fbi102
Loreau, M., De Mazancourt, C., 2008. Species synchrony and its drivers: neutral and nonneutral community dynamics in fluctuating environments. The American Naturalist 172, E48–E66. https://doi.org/10.1086/589746

Lorenzen, C.J., 1966. A method for the continuous measurement of *in vivo* chlorophyll concentration. Deep Sea Research 13, 223–227. https://doi.org/10.1016/0011-7471(66)91102-8
Mackas, D.L., Tsuda, A., 1999. Mesozooplankton in the eastern and western subarctic Pacific: community structure, seasonal life histories, and interannual variability. Progress in Oceanography 43, 335–363. https://doi.org/10.1016/S0079-6611(99)00012-9
Marcus, N.H., 1990. Calanoid copepod, cladoceran, and rotifer eggs in sea-bottom sediments of northern Californian coastal waters: Identification, occurrence and hatching. Marine Biology 105, 413–418. https://doi.org/10.1007/BF01316312
Matthews, S.A., Goetze, E., Ohman, M.D., 2021. Recommendations for interpreting zooplankton metabarcoding and integrating molecular methods with morphological analyses. ICES Journal of Marine Science 78, 3387–3396. https://doi.org/10.1093/icesjms/fsab107
Mauchline, J., 1998. The biology of calanoid copepods, Advances in Marine Biology. Academic Press, San Diego.
McKinstry, C.A.E., Campbell, R.W., 2018. Seasonal variation of zooplankton abundance and community structure in Prince William Sound, Alaska, 2009–2016. Deep Sea Research Part II: Topical Studies in Oceanography 147, 69–78. https://doi.org/10.1016/j.dsr2.2017.08.016
Menden-Deuer, S., Lessard, E.J., 2000. Carbon to volume relationships for dinoflagellates, diatoms, and other protist plankton. Limnology and Oceanography 45, 569–579. https://doi.org/10.4319/lo.2000.45.3.0569
Miller, C.B., Clemons, M.J., 1988. Revised life history analysis for large grazing copepods in the subarctic Pacific Ocean. Progress in Oceanography 20, 293–313.
Miller, C.B., Frost, B.W., Batchelder, H.P., Clemons, M.J., Conway, R.E., 1984. Life histories of large, grazing copepods in a subarctic ocean gyre: *Neocalanus plumchrus*, *Neocalanus cristatus*, and *Eucalanus bungii* in the northeast Pacific. Progress in Oceanography 13, 201–243. https://doi.org/10.1016/0079-6611(84)90009-0
Monell, K.J., Roncalli, V., Hopcroft, R.R., Hartline, D.K., Lenz, P.H., 2023. Post-diapause DNA replication during oogenesis in a capital-breeding copepod. Integrative Organismal Biology 5, 1–17. https://doi.org/10.1093/iob/obad020
Mueter, F.J., Norcross, B.L., 2002. Spatial and temporal patterns in the demersal fish community on the shelf and upper slope regions of the Gulf of Alaska. Fish Bulletin 100, 559–581.
Nakatani, T., 1995. Monthly changes in density and size structure of copepod nauplii as the primary food for fish larvae in winter in Funka Bay and surrounding vicinity in Hokkaido. Fisheries Science 61, 382–386.
Napp, J.M., Hopcroft, R.R., Baier, C.T., Clarke, C., 2005. Distribution and species-specific egg production of *Pseudocalanus* in the Gulf of Alaska. Journal of Plankton Research 27, 415–426. https://doi.org/10.1093/plankt/fbi015
Nichols, J.H., Thompson, A.B., 1991. Mesh selection of copepodite and nauplius stages of four calanoid copepod species. Journal of Plankton Research 13, 661–671. https://doi.org/10.1093/plankt/13.3.661
Niehoff, B., Madsen, S., Hansen, B., Nielsen, T., 2002. Reproductive cycles of three dominant *Calanus* species in Disko Bay, West Greenland. Marine Biology 140, 567–576. https://doi.org/10.1007/s00227-001-0731-3
Nielsen, J.M., Rogers, L.A., Brodeur, R.D., Thompson, A.R., Auth, T.D., Deary, A.L., Duffy-Anderson, J.T., Galbraith, M., Koslow, J.A., Perry, R.I., 2021. Responses of ichthyoplankton assemblages to the recent marine heatwave and previous climate fluctuations in several northeast Pacific marine ecosystems. Global Change Biology 27, 506–520. https://doi.org/10.1111/gcb.15415

Nishibe, Y., Ikeda, T., 2006. Vertical distribution, population structure and life cycles of four oncaeid copepods in the Oyashio region, western subarctic Pacific. Marine Biology 150, 609–625. https://doi.org/10.1007/s00227-006-0382-5
Nishida, S., 1985. Taxonomy and distribution of the family Oithonidae (Copepoda, Cyclopoida) in the Pacific and Indian oceans. Bulletin of Ocean Research 20, 1–167.
Norrbin, M.F., 2001. Ultra-structural changes in the reproductive system of overwintering females of *Acartia longiremis*. Marine Biology 139, 697–704. https://doi.org/10.1007/s002270100627
Norrbin, M.F., 1996. Timing of diapause in relation to the onset of winter in the high-latitude copepods *Pseudocalanus acuspes* and *Acartia longiremis*. Marine Ecology Progress Series 142, 99–109. https://doi.org/10.3354/meps142099
Norrbin, M.F., 1994. Seasonal patterns in gonad maturation, sex ratio and size in some small, high-latitude copepods: implications for overwintering tactics. Journal of Plankton Research 16, 115–131. https://doi.org/10.1093/plankt/16.2.115
O'Hara, M., 2023. Distribution and mixotrophy of cryptophyte phytoplankton in the northern Gulf of Alaska (Master's Thesis). Western Washington University.
Oksanen, J., Simpson, G.L., Blanchet, F.G., Kindt, R., Legendre, P., Minchin, P.R., O'Hara, R.B., Solymos, P., Stevens, M.H.H., Szoecs, E., Wagner, H., Barbour, M., Bedward, M., Bolker, B., Borcard, D., Carvalho, G., Chirico, M., Caceres, M.D., Durand, S., Evangelista, H.B.A., FitzJohn, R., Friendly, M., Furneaux, B., Hannigan, G., Hill, M.O., Lahti, L., McGlinn, D., Ouellette, M.-H., Cunha, E.R., Smith, T., Stier, A., Braak, C.J.F.T., Weedon, J., 2022. vegan: Community ecology package.
O'Rourke, D.R., Bokulich, N.A., Jusino, M.A., MacManes, M.D., Foster, J.T., 2020. A total crapshoot? Evaluating bioinformatic decisions in animal diet metabarcoding analyses. Ecology and Evolution 10, 9721–9739. https://doi.org/10.1002/ece3.6594
Paul, A.J., Paul, J.M., Coyle, K.O., Smith, R., 1991. Phytoplankton, zooplankton, and ichthyoplankton in Resurrection Bay, northern Gulf of Alaska in 1988 (No. 91– 02), Alaska Sea Grant College Program. University of Alaska Fairbanks.
Peters, J., Dutz, J., Hagen, W., 2013. Trophodynamics and life-cycle strategies of the copepods *Temora longicornis* and *Acartia longiremis* in the central Baltic Sea. Journal of Plankton Research 35, 595–609. https://doi.org/10.1093/plankt/fbt004
Peterson, W., 1979. Life history and ecology of *Calanus marshallae* Frost in the Oregon upwelling zone. Oregon State University.
Peterson, W.T., Tiselius, P., Kiørboe, T., 1991. Copepod egg production, molting and growth rates, and secondary production, in the Skagerrak in August 1988. Journal of Plankton Research 13, 131–154. https://doi.org/10.1093/plankt/13.1.131
Questel, J.M., Hopcroft, R.R., DeHart, H.M., Smoot, C.A., Kosobokova, K.N., Bucklin, A., 2021. Metabarcoding of zooplankton diversity within the Chukchi Borderland, Arctic Ocean: improved resolution from multi-gene markers and region-specific DNA databases. Marine Biodiversity 51, 1–19. https://doi.org/10.1007/s12526-020-01136-x
Ratnasingham, S., Herbert, P.D.N., 2007. BOLD: The barcode of life data system (www.barcodinglife.org). Molecular Ecology Notes 7, 355–364.
Record, N.R., Ji, R., Maps, F., Varpe, Ø., Runge, J.A., Petrik, C.M., Johns, D., 2018. Copepod diapause and the biogeography of the marine lipidscape. Journal of Biogeography 45, 2238–2251. https://doi.org/10.1111/jbi.13414
Renner, M., Arimitsu, M.L., Piatt, J.F., 2012. Structure of marine predator and prey communities along environmental gradients in a glaciated fjord. Canadian Journal of Fisheries and Aquatic Sciences 69, 2029–2045. https://doi.org/10.1139/f2012-117
Robinson, M.S., O'Rourke, D.R., Kaehler, B.D., Ziemski, M., Dillon, M.R., Foster, J.T., Bokulich, N.A., 2021. RESCRIPt: Reproducible sequence taxonomy reference database

management. PLOS Computational Biology 17, e1009581. https://doi.org/10.1371/journal.pcbi.1009581
Rogers, L.A., Dougherty, A.B., 2019. Effects of climate and demography on reproductive phenology of a harvested marine fish population. Global Change Biology 25, 708–720. https://doi.org/10.1111/gcb.14483
Rognes, T., Flouri, T., Nichols, B., Quince, C., Mahé, F., 2016. VSEARCH: a versatile open source tool for metagenomics. PeerJ 4, e2584. https://doi.org/10.7717/peerj.2584
Roncalli, V., Block, L.N., Niestroy, J.L., Cieslak, M.C., Castelfranco, A.M., Hartline, D.K., Lenz, P.H., 2023. Experimental analysis of development, lipid accumulation and gene expression in a high-latitude marine copepod. Journal of Plankton Research 45, 885–898. https://doi.org/10.1093/plankt/fbad045
Roncalli, V., Cieslak, M.C., Castelfranco, A.M., Hartline, D.K., Lenz, P.H., 2022. Postponing development: dormancy in the earliest developmental stages of a high-latitude calanoid copepod. Journal of Plankton Research 44, 923–935. https://doi.org/10.1093/plankt/fbac039
Roncalli, V., Cieslak, M.C., Hopcroft, R.R., Lenz, P.H., 2020. Capital breeding in a diapausing copepod: A transcriptomics analysis. Frontiers in Marine Science 7, 56.
Royer, T.C., 1974. Seasonal variations of waters in the northern Gulf of Alaska. Deep-Sea Research 22, 403–416.
Sainmont, J., Andersen, K.H., Varpe, Ø., Visser, A.W., 2014. Capital versus income breeding in a seasonal environment. The American Naturalist 184, 466–476. https://doi.org/10.1086/677926
Saito, H., Tsuda, A., 2000. Egg production and early development of the subarctic copepods *Neocalanus cristatus*, *N. plumchrus* and *N. flemingeri*. Deep Sea Research Part I: Oceanographic Research Papers 47, 2141–2158. https://doi.org/10.1016/S0967-0637(00)00017-0
Schindler, D.E., Armstrong, J.B., Reed, T.E., 2015. The portfolio concept in ecology and evolution. Frontiers in Ecology and the Environment 13, 257–263. https://doi.org/10.1890/140275
Schoener, T.W., 1974. Resource Partitioning in Ecological Communities. Science 185, 27–39. https://doi.org/10.1126/science.185.4145.27
Selph, K.E., 2021. Enumeration of marine microbial organisms by flow cytometry using near-UV excitation of Hoechst 34580-stained DNA. Limnology and Oceanography: Methods 19, 692–701. https://doi.org/10.1002/lom3.10454
Slater, L.M., 2004. Development, growth, and egg production of *Centropages abdominalis* and *Neocalanus flemingeri* from the eastern subarctic Pacific. University of Alaska Fairbanks.
Sousa, L., Coyle, K.O., Barry, R.P., Weingartner, T.J., Hopcroft, R.R., 2016. Climate-related variability in abundance of mesozooplankton in the northern Gulf of Alaska 1998–2009. Deep Sea Research Part II: Topical Studies in Oceanography, Understanding Ecosystem Processes in the Gulf of Alaska: Volume 1 132, 122–135. https://doi.org/10.1016/j.dsr2.2016.04.006
Stabeno, P.J., Bond, N.A., Hermann, A.J., Kachel, N.B., Mordy, C.W., Overland, J.E., 2004. Meteorology and oceanography of the northern Gulf of Alaska. Continental Shelf Research 24, 859–897. https://doi.org/10.1016/j.csr.2004.02.007
Steinberg, D.K., Landry, M.R., 2017. Zooplankton and the ocean carbon cycle. Annual Review of Marine Science 9, 413–444. https://doi.org/10.1146/annurev-marine-010814-015924
Strom, S., Olson, M., Macri, E., Mord, C., 2006. Cross-shelf gradients in phytoplankton community structure, nutrient utilization, and growth rate in the coastal Gulf of Alaska. Marine Ecology Progress Series 328, 75–92. https://doi.org/10.3354/meps328075
Strom, S.L., Fredrickson, K.A., Bright, K.J., 2019. Microzooplankton in the coastal Gulf of Alaska: Regional, seasonal and interannual variations. Deep Sea Research Part II:

Topical Studies in Oceanography 165, 192–202. https://doi.org/10.1016/j.dsr2.2018.07.012
Strom, S.L., Fredrickson, K.A., Bright, K.J., 2016. Spring phytoplankton in the eastern coastal Gulf of Alaska: Photosynthesis and production during high and low bloom years. Deep Sea Research Part II: Topical Studies in Oceanography 132, 107–121. https://doi.org/10.1016/j.dsr2.2015.05.003
Sverdrup, H.U., 1953. On conditions for the vernal blooming of phytoplankton. ICES Journal of Marine Science 18, 287–295. https://doi.org/10.1093/icesjms/18.3.287
Takahashi, K., Kuwata, A., Sugisaki, H., Uchikawa, K., Saito, H., 2009. Downward carbon transport by diel vertical migration of the copepods *Metridia pacifica* and *Metridia okhotensis* in the Oyashio region of the western subarctic Pacific Ocean. Deep Sea Research Part I: Oceanographic Research Papers 56, 1777–1791. https://doi.org/10.1016/j.dsr.2009.05.006
Takahashi, T., Uchiyama, I., 2007. Morphology of the naupliar stages of some Oithona species (Copepoda: Cyclopoida) occurring in Toyama Bay, southern Japan Sea. Plankton and Benthos Research 2, 12–27. https://doi.org/10.3800/pbr.2.12
Tilman, D., 1996. Biodiversity: Population versus ecosystem stability. Ecology 77, 350–363. https://doi.org/10.2307/2265614
Tsuda, A., Saito, H., Kasai, H., 1999. Life histories of *Neocalanus flemingeri* and *Neocalanus plumchrus* (Calanoida: Copepoda) in the western subarctic Pacific. Marine Biology 135, 533–544. https://doi.org/10.1007/s002270050654
Varpe, Ø., Jørgensen, C., Tarling, G.A., Fiksen, Ø., 2009. The adaptive value of energy storage and capital breeding in seasonal environments. Oikos 118, 363–370. https://doi.org/10.1111/j.1600-0706.2008.17036.x
Vidal, J., Smith, S.L., 1986. Biomass, growth, and development of populations of herbivorous zooplankton in the southeastern Bering Sea during spring. Deep Sea Research Part A. Oceanographic Research Papers 33, 523–556. https://doi.org/10.1016/0198-0149(86)90129-9
Waite, J.N., Mueter, F.J., 2013. Spatial and temporal variability of chlorophyll *a* concentrations in the coastal Gulf of Alaska, 1998–2011, using cloud-free reconstructions of SeaWiFS and MODIS-Aqua data. Progress in Oceanography 116, 179–192. https://doi.org/10.1016/j.pocean.2013.07.006
Wiborg, K.F., 1954. Investigations on zooplankton in coastal and offshore waters of western and northwestern Norway - with special reference to the copepods (Report of Norwegian Fishery and Marine Investigations).
Wickham, H., Averick, M., Bryan, J., Chang, W., McGowan, L., François, R., Grolemund, G., Hayes, A., Henry, L., Hester, J., Kuhn, M., Pedersen, T., Miller, E., Bache, S., Müller, K., Ooms, J., Robinson, D., Seidel, D., Spinu, V., Takahashi, K., Vaughan, D., Wilke, C., Woo, K., Yutani, H., 2019. Welcome to the tidyverse. JOSS 4, 1–6. https://doi.org/10.21105/joss.01686
Wong, C.K., 1988. Effects of competitors, predators, and prey on the grazing behavior of herbivorous Calanoid copepods. Bulletin of Marine Science 43, 573–582.
Xu, S., Chen, M., Feng, T., Zhan, L., Zhou, L., Yu, G., 2021. Use ggbreak to effectively utilize plotting space to deal with large datasets and outliers. Frontiers in Genetics 12, 1–7. https://doi.org/10.3389/fgene.2021.774846
Yamaguchi, A., Watanabe, Y., Ishida, H., Harimoto, T., Furusawa, K., Suzuki, S., Ishizaka, J., Ikeda, T., Takahashi, M.M., 2002. Community and trophic structures of pelagic copepods down to greater depths in the western subarctic Pacific (WEST-COSMIC). Deep Sea Research Part I: Oceanographic Research Papers 49, 1007–1025. https://doi.org/10.1016/S0967-0637(02)00008-0

Zamora-Terol, S., Nielsen, T., Saiz, E., 2013. Plankton community structure and role of *Oithona similis* on the western coast of Greenland during the winter-spring transition. Marine Ecology Progress Series 483, 85–102. https://doi.org/10.3354/meps10288

[1] *Oithona atlantica* has not been previously reported in the northern Gulf of Alaska region (Coyle and Pinchuk, 2003, Hopcroft and Clarke Hopcroft, 2019; Hopcroft, 2021, Sousa et al. 2016). However, DNA sequences from bulk community and naupliar cohort samples match with 100% identity to established *O. atlantica* sequences (Bucklin et al., 2021; Ratnasingham and Herbert, 2007). Historically, *Oithona similis* and *Oithona spinirostris* have been identified in the Gulf of Alaska based on Gardner and Szabo (1982), however the identity of *O. spinirostris* has been confused in the literature, with possible identifications to *O. atlantica* or *Oithona setigera* (Nishida, 1985). The identification of *O. spinirostris* in the Gulf of Alaska is currently under review. Herein, the species will be referred to as *O. spinirostris* when identified morphologically and *O. atlantica* when identified by DNA barcodes until the identity is confirmed.